Evaluation of high-rise building-based hydroelectric systems for improving energy efficiency at the urban scale

by

Tristan Walker

A thesis submitted to the Faculty of Graduate and Postdoctoral Affairs in partial fulfillment of the requirements for the degree of

Master of Applied Science

in

Sustainable Energy

Carleton University
Ottawa, Ontario

Abstract

This thesis assesses the potential benefits of implementing two alternative building-based hydroelectric technologies that have the capacity to improve energy efficiency at an urban scale. These technologies include a building-based hydroelectric system driven by wastewater, and the following two building-based hydroelectric energy storage systems: a pumped hydro system, and a gravity module system. An investigation is undertaken to analyze the techno-economic tradeoffs of each technology via the development of numerical models and their corresponding system scenarios. Results show that implementing a building-based wastewater hydroelectric system can offset the total annual pumping energy requirement by up to 36% regardless of the building's height, and that this system is cost effective when installed in buildings that have a minimum of 35 floors (roughly 105 m in height) and at least 47 units per floor. Regarding the two building-based hydroelectric energy storage systems, results show that the building-based gravity module system is capable of offering greater power capacity at a lower levelized electricity cost than the building-based pumped hydro system. The gravity module system can provide single-cycle storage capacities as high as 1,358 kWh in buildings that are 300 m tall. Moreover, this system, when used for energy storage purposes, has a lower levelized electricity cost than that of an equivalent lithium-ion battery system in all buildings exceeding 156 m in height.

Preface

This integrated thesis consists of two journal articles, which are currently under review. Should readers wish to reference materials from this thesis, the current thesis is required to be cited. The articles in this thesis are as follows:

- **Article 1:** T. Walker, and J. Duquette, (2021) "Performance evaluation of a residential building-based hydroelectric system driven by wastewater," *Sustainable Cities and Society* [Under Review]
- **Article 2:** T. Walker, and J. Duquette, (2021) "Evaluation of building-based hydroelectric systems as a rapidly deployable grid-scale energy storage solution," *Journal of Energy Storage* [Under Review]

The aforementioned articles have been adapted slightly in each corresponding chapter for ease of flow of the dissertation. The use of copyrighted material from the published articles is acknowledged as per the corresponding publisher's permissions guidelines with respect to the authors' rights.

Acknowledgements

Above all else I would like to thank my supervisor and role model Prof. Jean Duquette. During our time working together, your influence, patience, and insight has been critical to my development in writing and research, and my personal growth. I would also like to thank my research partners Shelby Hagerman and Lauren Johnson, as well as Professors Zach Colbert and Alex Mallet, for your positivity and work on this project. Furthermore, I would like to thank my friends and family for their continued support throughout; specifically, my Mom for inspiring me to always stay positive and persevere, and to my Dad and Sister for continuing to carry on that example. Finally, I would like to acknowledge and thank the Government of Canada's New Frontiers in Research Fund for providing funding for this project.

Nomenclature

Symbols	
A	Area of the base of the steel piston (m^2)
C_c	Capital cost ($)*
C_{co}	Capital cost of the concrete containment column ($)*
c_j	Annual operations and maintenance cost ($/yr)*
c_{LIBP}	Annual variable system cost of lithium-ion battery plant ($/yr)*
c_m	Pump maintenance cost ($/MWh/yr)*
c_{NGPP}	Annual variable system cost of natural gas power plant ($/yr)*
C_p	Capital cost of pumping system ($)*
c_p	Annual variable pump cost ($/yr)*
C_{pe}	Capital cost of the penstock ($)*
C_r	Capital cost of pumped hydro reservoir ($)*
C_s	Capital cost of steel piston ($)*
C_{se}	Variable storage cost ($/kWh)*
C_t	Capital cost of turbine and electromechanical equipment ($)*
c_t	Annual variable turbine cost ($/yr)*
d	Penstock diameter (m)
$d_{tank_{out}}$	Pipe diameter below the collection tank (m)
$d_{pump_{PZ}}$	Pipe diameter supplying pressure zone (m)
E_{cycle}	Energy cycle capacity (*i.e.,* energy stored over a single cycle) (kWh)
E_p	Pump energy consumption per time step (Wh)
$E_{p_{annual}}$	Annual pumping energy consumption (kWh)
$E_{pump}(t)$	Energy used by the pumping system (kWh)
E_t	Turbine energy generation per timestep (Wh)
$E_{t_{annual}}$	Annual turbine energy generation (kWh)
$E_{turbine}(t)$	Energy generated by the turbine-generator assembly (kWh)
e	Pipe roughness (m)
f	Friction factor
$f_{pump_{PZ}}(t)$	Friction factor corresponding to pressure zone
$f_{tank_{out}}(t)$	Friction factor corresponding to turbine system
g	Gravitational constant (9.81 m^2/s)
H	Equivalent gross head of water (m)
ΔH_p	Total head for the pumping system (m)
$\Delta H_{pump}(t)$	Change in head of the pumping system (m)
$\Delta H_{pump_{PZ}}(t)$	Change in head of pressure zone (m)
ΔH_t	Total head for the turbine system (m)
$\Delta H_{turbine}$	Change in head of the turbine (m)
HR	Heat rate (GJ/kWh)
i	Discount rate (%)
j	Current year

k	Project Lifetime (yrs)
L	Length of penstock (m)
m_{steel}	Mass of the steel piston (kg)
m_{water}	Mass of the volume of water equivalent to that of the steel piston (kg)
$\dot{m}$	Mass flow rate (kg/s)
$\dot{m}_{pump_{in}}(t)$	Mass flow rate of flow entering the building (kg/s)
$\dot{m}_{tank_{in}}(t)$	Mass flow rate of effluent entering the collection tank (kg/s)
$\dot{m}_{tank_{out}}(t)$	Mass flow rate of effluent exiting the collection tank (kg/s)
Ns	Specific speed
ΔP	System pressure differential (Pa)
P_{steel}	Pressure exerted by the steel piston (Pa)
P_{water}	Pressure exerted by volume of water equivalent to that of the steel piston (Pa)
Q	Volumetric flowrate (m^3/s)
r_E	Electricity rate used for energy storage ($/kWh)*
r_{elec}	Electricity rate used for wastewater turbine ($/kWh)*
r_{NG}	Natural gas rate ($/GJ)*
R_j	Annual turbine energy revenue ($/yr)*
Re	Reynolds number
$Re_{pump_{PZ_1}}(t)$	Reynolds number corresponding to pressure zone
$Re_{tank_{out}}(t)$	Reynolds number corresponding to turbine system
Δt	Timestep (s)
$u_{tank_{out}}(t)$	Velocity of effluent leaving the collection tank (m/s)
$u_{pump_{PZ}}(t)$	Velocity of water being pumped in pressure zone (m/s)
V	Fluid velocity (m/s)
$V_{tank}(t)$	Volume of effluent in the collection tank (m^3)
W_p	Pump power consumption per time step (W)
$\dot{W}_{pump}(t)$	Power consumed by the pump (kW)
W_t	Turbine power generation per time step (W)
$\dot{W}_{turbine}(t)$	Power generated by the turbine-generator assembly (kW)
Δz_{PZ}	Height of pressure zone (m)

* The Canadian dollar (CAD) currency is utilized for all costs in the current study. All American dollar (USD) and Euro (EUR) values have been adjusted to Canadian dollars using an exchange rate of 1.33 CAD/USD, and 1.52 CAD/EUR, respectively [1].

Abbreviations and Acronyms	
BBPH	Building-based pumped hydro
BBGM	Building-based gravity module
CRF	Capital recovery factor
EIA	Energy Information Administration
ER	Energy ratio
FES	Future Energy Shift
hrs	Hours
LEC	Levelized electricity cost
LIBP	Lithium-ion battery plant
NGPP	Natural gas peaker plant
NPC	Net present cost
NPV	Net present value
O&M	Operations and maintenance
RTP	Real time pricing
TOU	Time of use

Greek letters	
η_{LIBP}	Round trip efficiency of lithium-ion battery plant (%)
η_{pump}	Efficiency of the pumping system in wastewater hydroelectric study (%)
η_p	Total efficiency of the energy storage pumping system (%)
$\eta_{turbine}$	Efficiency of the turbine-generator assembly in wastewater hydroelectric study (%)
η_t	Total efficiency of the energy storage turbine-generator assembly (%)
σ_{cycle}	Time for single pumping and generation cycle (hrs)
ω	Rotational speed (rpm)
ρ_s	Density of steel (7,871 kg/m^3)
ρ_{water}	Density of water (997 kg/m^3)
μ_{water}	Dynamic viscosity of water (0.00143 Ns/m^3)

Table of Contents

List of Tables

List of Figures

Foreword

This thesis was undertaken as part of the interdisciplinary Future Energy Shift (FES) research program, comprised of researchers in the fields of Engineering, Architecture, and Public Policy, to determine the feasibility of using the existing urban building stock for electrical energy generation and storage. The students and professors involved include myself and Prof. Jean Duquette (Engineering), Shelby Hagerman and Prof. Zach Colbert (Architecture), and Lauren Johnson and Prof. Alex Mallet (Policy), respectively.

The above-mentioned group worked collaboratively over the course of two-and-a-half years to gather and analyze both quantitative and qualitative data from a variety of sources. The quantitative data mainly included structural drawings, and water and electrical consumption data for a number of buildings located in Ottawa (obtained from the Mondrian residential building, and a subset of Ottawa Community Housing buildings), and Vancouver (obtained from a number of buildings via the Condominium Home Owners Association of British Columbia). The qualitative data included information gathered from multiple surveys, interviews, building site visits, and focus groups with residents living in these buildings.

It is important to note that the current project was significantly impacted by the onset of the COVID-19 pandemic only a few months after it officially began. At that time, all planned in-person activities (such as building site visits, and field work in Vancouver) were cancelled and the project was forced to move to a fully virtual format. Despite this setback, the students continued to meet online on a regular basis which allowed the different disciplines to share and integrate their findings, discuss the possible challenges

they had encountered, and also to identify potential solutions to address these challenges. Throughout this process, the FES team developed a strong sense of interdisciplinarity and saw an opportunity to leverage their experiences and create a tool that may be of value to other groups working under similar conditions. This tool consists of an interactive graphic of the building design timeline that the group utilized as a central discussion piece throughout their research. It was used effectively in a focus group comprised of students in the fields of engineering, architecture, and public policy, and recently showcased (as a presentation, and a research article) in the following high-impact cross-disciplinary conference:

Conference article:

- L. Johnson, S. Hagerman, T. Walker, D. Dickson, E. Stone, Z. Colbert, A. Mallett, J. Duquette, "An interdisciplinary timeline: A roadmap to operationalize interdisciplinarity," in *Proc. of CUNY Cities in a Changing World: Questions of culture, climate, and design,* New York, USA, held online, 2021. [Accepted]

Conference presentation:

- L. Johnson, S. Hagerman, T. Walker, "The interdisciplinary timeline," presented at *Proc. of CUNY Cities in a Changing World: Questions of culture, climate, and design,* New York, USA, held online, 2021.

From an engineering standpoint, the project resulted in the following journal articles, which are currently under review:

Journal articles:

- T. Walker, and J. Duquette, (2021) "Performance evaluation of a residential building-based hydroelectric system driven by wastewater," *Sustainable Cities and Society* [Under Review]
- T. Walker, and J. Duquette, (2021) "Evaluation of building-based hydroelectric systems as a rapidly deployable grid-scale energy storage solution," *Journal of Energy Storage* [Under Review]

Chapter 1: Introduction

In this thesis two alternative high-rise building-based hydroelectric generation systems are proposed for the purpose of improving energy efficiency at an urban scale. These systems include a building-based hydroelectric system driven by wastewater, and the following two building-based hydroelectric energy storage systems: a pumped hydro system, and a gravity module system. The rationale for investigating each of the systems mentioned above are described in the following sub-sections:

1.1 Rationale for investigating building-based hydroelectric systems driven by wastewater

A considerable amount of energy is wasted each year in high-rise residential buildings worldwide as a result of domestic water being flushed or poured down drains by the buildings' occupants [2]. Wastewater located on any given floor in a building contains potential energy that in theory may be harnessed as it makes its way toward the sewer via gravity drainage; and the greater the elevation of the floor, the greater the potential available for harnessing this energy. However, as the elevation of a building increases, the energy that is required to pump domestic water to the point where the wastewater originates also increases in a proportional manner [3]. Therefore, harnessing wastewater energy from any building, no matter its height, can at best only serve to recover a portion of the initial energy expended to distribute water to all the building's fixtures, thereby increasing the energy efficiency of the domestic water distribution system. Energy recovery in the context described above can only occur if an adequate power generation system such as a small hydro turbine-generator system is installed in the building's main wastewater outflow pipe. The operation of such a system, when combined with the building's domestic water

distribution system, is analogous to that of a conventional pumped hydroelectric system [4], with the exception that no storage capacity is available, and all pumping/generation events occur intermittently based on occupant loads.

1.2 Rationale for investigating building-based pumped hydro and gravity module systems

With the growing global emergence of intermittent renewable generation technologies in power grids comes the need for increased capacity of grid-scale energy storage solutions that provide power regulation services [5]. It is estimated that every kWh of renewable energy generated requires between 5 and 15 Wh of energy storage [6]. The most common and mature grid-scale energy storage technology to date is pumped hydro, which uses a pump-turbine assembly to displace water between two large reservoirs separated by an elevation drop [7]. Energy is stored when water is pumped from the lower reservoir to the upper reservoir, and energy is generated when this direction is switched. Although more than 161 GW of capacity is currently in operation worldwide [5,6], finding new potential sites for these installations is challenging mainly due to the scarce availability of natural waterways situated in proximity to acceptable elevation gradients, and the technical and environmental limitations associated with building a facility in these locations [10]. Pumped hydro storage plants can also be developed in the absence of natural waterways, so long as a significant elevation drop is present. However, this option is rarely considered due to the considerable material requirements for building the plants, and the exorbitant associated capital cost. For example, storing 6 GWh/day over a 400 m height difference requires roughly 72 hectares of land, and over 6 gigalitres of water (not including

the annual makeup water required due to evaporation losses) and can cost upwards of $1.2 billion [11].

As an alternative to the large-scale pumped hydro options listed above, this thesis investigates two smaller scale hydroelectric storage system options that are building-centered. These options include a building-based pumped hydro (BBPH) system, and a building-based gravity module (BBGM) system. A BBPH system operates in a similar fashion to its larger scale counterpart with the exception that the upper and lower reservoirs consist of tanks located on a building's roof and ground level, respectively. A BBGM system, on the other hand, consists of one or more water-filled vertical columns spanning the height of a building where each column includes an internal piston made of a high-density material like steel. An external water pipe connects the top and bottom of the column via a pump-turbine assembly. As the pump operates, the piston increases in height gaining potential energy. When the piston is released, the water under the piston is displaced through the turbine. High-rise buildings are ideally suited for siting these systems as: 1) the components can be integrated within the buildings' existing footprint thus avoiding the need for additional vacant land; 2) a suitable elevation drop is present; and 3) most buildings in a city are located in close proximity to water and electricity distribution lines which drastically lowers the cost of implementation. Additional benefits of BBPH and BBGM systems include the availability of integrated fire protection for buildings, and ancillary services to the electrical grid such as contingency reserves, emergency power to critical services, and flexibility reserves. Moreover, these systems can also provide peak load shaving services which helps to reduce congestion in transmission and distribution

power lines [9,2]. These benefits have the potential to increase considerably if the proposed systems are interconnected and expanded into a city-wide distributed network.

1.3 Overview of building-based hydroelectric system modeling studies

The following sub-sections provide a review of the literature surrounding high-rise building-based hydroelectric systems, as well as a summary of the research gaps identified for each system type.

1.3.1 Building-based hydroelectric systems driven by wastewater

Very few studies have been conducted on the topic of building-based wastewater hydroelectric systems. In one study, Sarkar et al. developed a numerical model of a system comprising a Pelton turbine at ground-level connected to a 32.4 m^3 greywater collection tank situated on the 10^{th} floor of a twenty-story case study building in India [13]. They found that with an available height difference of 28.3 m between a 2.5 kW turbine and the tank, approximately 6.85 kWh of electricity could be generated on a daily basis. Sarkar assumed 100 residents lived on each floor and each resident consumed 171 L of water per day, giving the system a flow rate of 11 L/s assuming it were deployed 4 times a day for 45 minutes. The total system cost was found to be $1,463 with a payback period of 7.7 years. It is expected that installing a similar system in a European or North American city would be significantly more costly. When they applied their model to a forty-story building (*i.e.*, a building that is twice the height of the case study building), they found that the energy generation could be increased roughly fourfold. Similarly, Titus & Ayalur, simulated a wastewater hydroelectric system in which a 741 W Pelton turbine was located 14 m below a 388 m^3 pretreated sewage collection tank [14]. They found that the system was capable of generating approximately 6 kWh of electricity per day assuming that the

tank discharged for 12 hours per day at a flow rate of 9 L/s, and that the total system cost amounted to $1,027 with a payback period of 6.7 years. In a separate study with a slightly different focus conducted on a building in Tucson, Arizona, Santillan developed a numerical model of a system that pumps wastewater from the building's main sewer outflow pipe to a 56.8 m^3 surge tank located on the building's top floor, 33.2 m above [2]. The system was only released during daily electricity grid peak power rate periods in order to maximize the cost savings. The study was conducted on an eleven-story case study building and assumed that 22 residents lived on each floor and each resident consumed 314 L of water per day. They found that when a Pelton turbine with a capacity of 1.06 kW was used, the system could generate approximately 4.25 kWh of electricity per day, assuming that the tank discharged for 4 hours per day at a flow rate of 3.9 L/s.

The numerical studies described above assess the performance of building-based wastewater hydroelectric systems using estimated daily averaged water consumption data for buildings of a fixed size, and contain limited information on the system's cost effectiveness. To the authors' knowledge, a detailed techno-economic performance analysis using measured water consumption data for these systems as a function of building size has not yet been conducted.

1.3.2 Building-based pumped hydro and gravity module systems

A limited number of works in the literature (only two to the authors' knowledge) are focused on assessing the potential techno-economic benefits of BBPH systems. Zhang et al. [15] conducted a study in which they modeled a proposed mini pumped hydro storage system installed in a high-rise building in Shanghai, China. They assumed the system operated with a head difference of 420 m between an upper and a lower tank (each with a

volume of 3,104 m^3), a constant flow rate of 0.7 m^3/s, a round trip electrical efficiency of 66%, and pump and generator rated capacities of 3,600 kW, and 2,400 kW, respectively. Their results show that the proposed system is economically viable if it is located in a jurisdiction where time-of-use pricing is available, and a minimum of three generation cycles are operated on a daily basis. In another study by Oliveira et al. [16], data from an experimental BBPH system located in the Goudemand residence complex in Arras, France was used to validate a techno-economic model of a proposed case study BBPH system. The existing building is 30 m tall and consists of a 60 m^3 tank located on the building's roof, and five 10 m^3 tanks located on the building's ground floor. The system is capable of generating up to 3.5 kWh of useful energy per cycle using a Pelton turbine rated at 450 W, and a centrifugal pump rated at 1.5 kW. The case study building, on the other hand, is 20 m tall and consists of an open 80 m^3 tank located on the building's roof, and an enclosed 80 m^3 tank located on the building's ground floor. Assuming a round trip efficiency of 35%, a power capacity of 1.5 kW and a peak energy storage capacity of 3.7 kWh, they determined the system's levelized electricity cost over a project lifetime of 25 years to be $5.46/kWh. This stated cost significantly exceeded that of the following two competing technologies they compared against in their study: lithium ion batteries ($0.68/kWh) and lead acid batteries ($1.9/kWh).

As in the case for BBPH systems, few studies in the literature are focused on assessing the potential techno-economic benefits of BBGM systems. In one related study, Ruoso et al. [17] developed a numerical model of a building-based gravity system that stores energy generated from a solar photovoltaic array using a motor and pulley system comprising a 12 m tall column of 4 m in diameter with an internal piston of 5 m in length

(instead of a water pump and turbine system, as in the case of BBGM systems). Their results showed that the system could store and generate approximately 11 kWh of energy over a discharge period of 30 minutes with an overall roundtrip efficiency of 90%. In a separate purely technically focused study, Loudiyi and Berrada [18] built a small-scale experimental BBGM system to be used for validating their numerical model. The 40 W capacity system consisted of a column measuring 2.2 m in height, and 0.6 m in diameter, and included a 0.67 m tall piston. They found that the system could store roughly 3.5 Wh of energy when a flow rate of 1.27×10^{-3} m^3/s, and a discharge time of 5.6 minutes were considered. The most complete techno-economic study on BBGM systems to date was conducted by Oldenmenger [6]. He modeled a baseline scenario that includes a single-column BBGM system located in the center of a fictitious 80 m tall building that uses a Francis turbine and pump configuration. The system consists of an 8.1 m diameter column spanning the height of the building and includes a 10 m tall piston. The system was found to be capable of storing up to 432 kWh of energy with a roundtrip efficiency of 69%, and has a generation capacity of 381 kW which can be sustained for roughly 55 minutes when a flow rate of 1.04 m^3/s is used. His findings revealed that the fixed and variable storage costs of the system were approximately $939/kW and $3,099/kWh, respectively. As part of the same study by Oldenmenger, a case study building scenario was modeled using the 160 m tall Torre Sofia located in San Pedro Garza Garcia, Mexico. A BBGM system identical to that used in the baseline scenario was used, that included a column tailored to the building's height. Additionally, the piston height was increased to 48 m. As a result, the energy storage capacity increased to roughly 3,331 kWh with a roundtrip efficiency of 74%, and the generation capacity increased to 3,200 kW and could be sustained for

approximately 55.5 minutes when a flow rate of 1.69 m^3/s was used. His findings showed that by implementing the BBGM system on a larger scale, storage costs decreased by nearly two thirds to $355/kW and $1,103/kWh relative to the baseline system.

The studies described above provide an assessment of the techno-economic performance of individual BBPH or BBGM energy storage systems, however, a direct comparison of these systems as a function of building height and system capacity has not been conducted; nor has a direct comparison been made between these systems and other conventional rapidly deployable grid-scale energy generation and/or storage technologies like natural gas peaker plants (NGPP), and lithium-ion battery plants (LIBP). NGPP plants (although not a storage technology) are currently used extensively, especially in North America to cover the vast majority of peak loads [19, 20], and LIBP plants are currently one of the most popular sources of new grid energy storage, accounting for roughly 51% of newly announced storage in 2015 [21].

1.4 Research Objectives

The research objectives addressed in this integrated thesis are broken down by chapter as follows to address the gaps in the literature outlined in Section 1.3:

- Chapter 2: Performance evaluation of a residential building-based hydroelectric system driven by wastewater:
    - Assess the techno-economic performance of a residential building-based wastewater hydroelectric system as a function of building size.
    - Identify a suitable dispatch strategy which may be used to control the proposed system based on the day of the week and the current state of charge of the wastewater collection tank.

- Chapter 3: Evaluation of high-rise building-based hydroelectric systems as an alternative rapidly deployable grid-scale energy storage solution:
    - Assess the techno-economic performance of both high-rise residential building-based gravity modules and building-based pumped hydro systems as a function of building height.
    - Compare the viability of these systems with other conventional rapidly deployable grid-scale energy generation and/or storage technologies like natural gas peaker plants (NGPP), and lithium-ion battery plants (LIBP).

1.5 Document Structure

The remainder of this integrated thesis consists of two main body chapters on 1) building-based hydroelectric systems driven by wastewater (Chapter 2), and 2) building-based hydroelectric energy storage systems (Chapter 3). Chapters 4-6 summarize the key research contributions of this thesis, present future research recommendations, and conclusions.

Chapter 2

This chapter has been submitted for publication as:

T. Walker, and J. Duquette, (2021) "Performance evaluation of a residential building-based hydroelectric system driven by wastewater," *Sustainable Cities and Society* [Under Review]

Chapter 2: Performance evaluation of a residential building-based hydroelectric system driven by wastewater

2.1 Introduction

In order to address the objectives outlined in Chapter 1, a numerical model of the proposed system is developed using the Matlab/Simscape™ tool. A 23-floor residential building located in Ottawa, Canada, is used as the case study in the analysis. Measured domestic water consumption data from the reference year 2019 is used as an input in the model. Model simulations are conducted using an hourly control strategy that varies its mode of operation depending on the day of the week and the volume of wastewater contained in the collection tank. System performance is quantified by calculating the annual turbine energy generation (MWh/year), and the net present value ($). Additionally, a sensitivity analysis is conducted to gauge the impact of varying the values of key system economic parameters. To assess the impact of building size on the proposed system's performance, scenarios of buildings comprising 15 to 75 floors, and 10 to 50 residential units/floor are analyzed, resulting in a total of 2,400 scenarios.

2.2 Methodology

The following sub-sections provide details regarding the case study building and proposed system model layout; as well as the modelling framework, scenarios, and performance metrics utilized in this study.

2.2.1 Case Study Building

A 70 m tall residential building located in Ottawa, Canada is used as the case study in the current work. The building, shown in Figure 2-1, comprises 23 floors each measuring 2.91 m in height. The lower 5 floors are used as a parking garage, and all other floors are used for residential purposes. The building has a total of 249 units, all of which are either one or two-bedroom suites, and approximately 378 residents. The average floor area is 996 m^2 and the total livable floor area is 35,856 m^2.

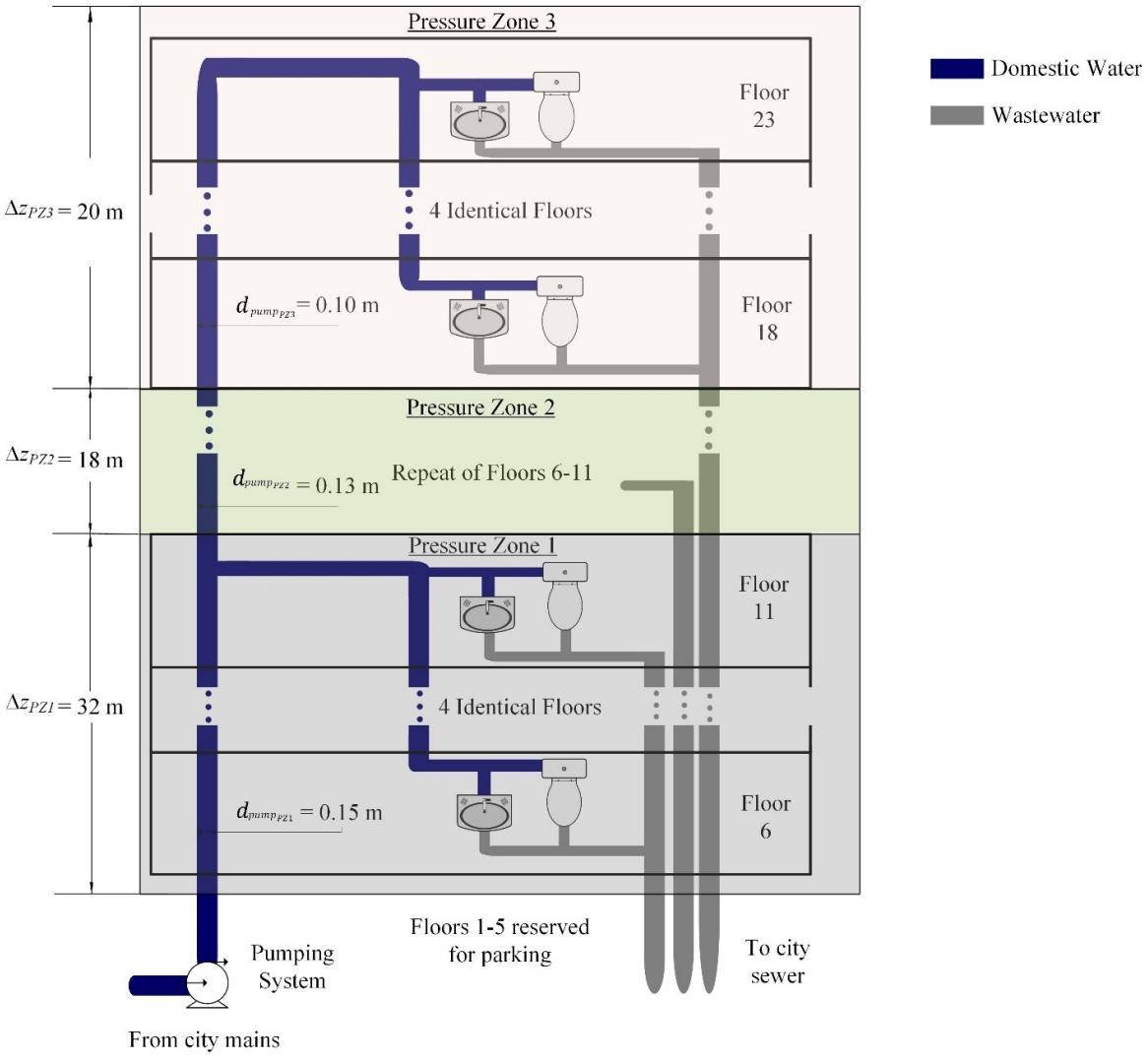

Figure 2-1: Layout of domestic water supply and wastewater distribution system in case study 23-floor residential building.

The building domestic water pumping system consists of a set of three pumps arranged in parallel. These pumps are exposed to a municipal supply pressure of approximately 275 kPa [22] and are operated to maintain a minimum fixture pressure of roughly 205 kPa [23] on the top floor of each pressure zone; the remaining floors below each pressure zone are supplied via gravity.

Each pressure zone is 6 floors high in order to keep the maximum pressure at the bottom of each zone below 480 kPa [24]. Once the domestic water (shown by blue lines in Figure 2-1) is consumed by residents at various fixture points such as toilets, sinks, and washing machines, it is converted to wastewater (shown by grey lines in Figure 2-1) and flows by gravity to the city sewer via one of three vertical stacks, each of which is associated with one of the three building pressure zones.

2.2.2 Wastewater hydroelectric system model

A Matlab/Simscape^{TM} model is developed to simulate the proposed building-based wastewater hydroelectric system, shown in Figure 2-2.

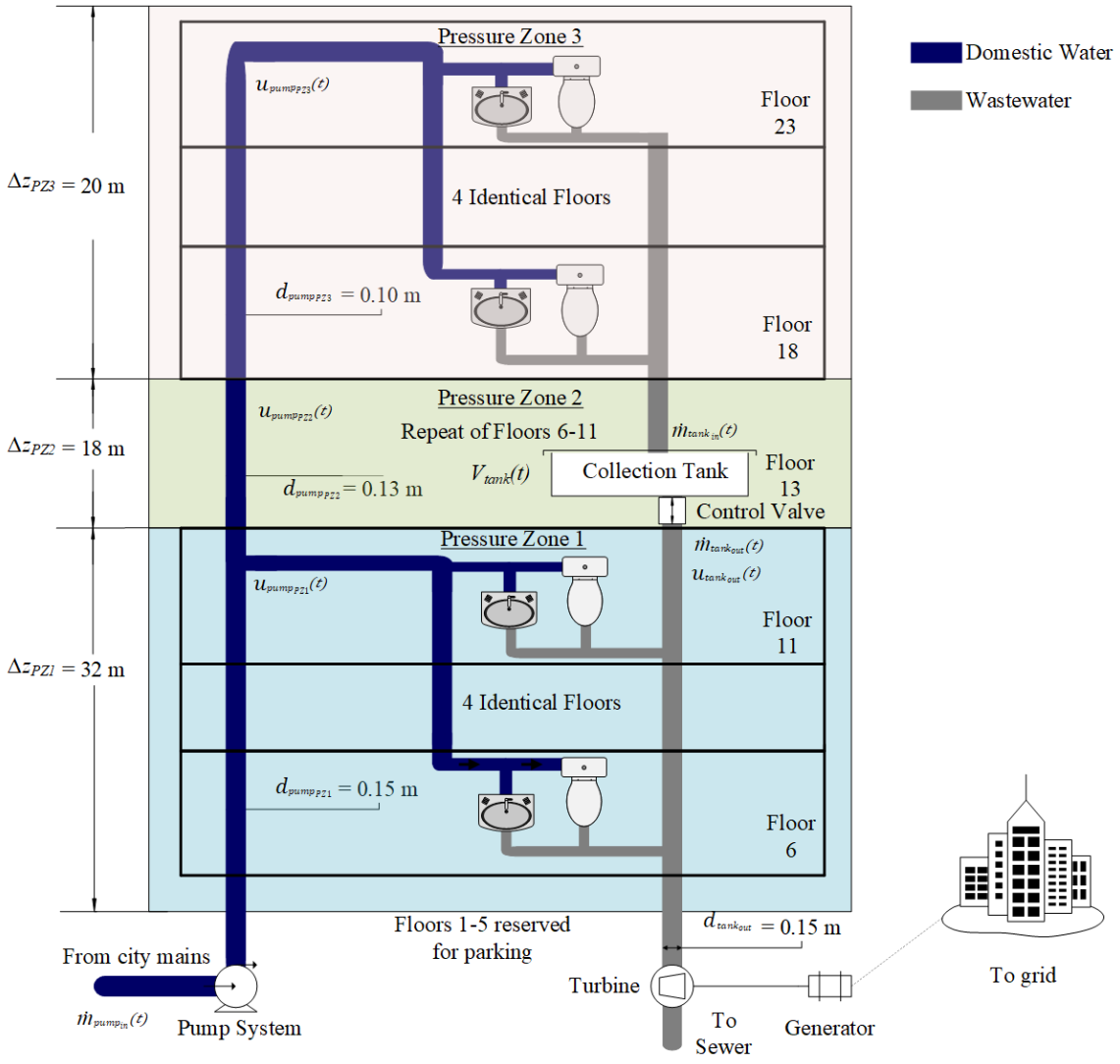

Figure 2-2: Schematic of case study building modified to include a wastewater collection tank and turbine-generator assembly for power generation.

The following assumptions are taken to develop the model:

- The domestic water pumping system consists of variable speed pumps that operate at constant efficiency;
- The pipe material is steel;

- Minor losses in the pipes and from fixtures and fittings are neglected, and friction losses from horizontal pipe lengths to supply domestic water to the units at each floor are ignored;
- A single vertical wastewater stack is used;
- Water is the working fluid (*i.e.,* potential solids contained in the wastewater are neglected);
- The total wastewater available for power generation purposes is equivalent to the total domestic water consumed by residents living on floors 13-23;
- A collection tank is used to store wastewater and controlled using a valve to ensure that the turbine-generator assembly can operate under nominal conditions. As the collection tank is the only controllable wastewater source that feeds the turbine-generator assembly, all wastewater stemming from floors located below the collection tank bypasses the turbine and is sent directly to the sewer.
- A 300 W Pelton turbine-generator assembly located at ground level is used to generate and deliver power to the electricity grid;
- The turbine-generator assembly operates at constant efficiency.

A preliminary analysis was conducted to identify the optimum wastewater tank location in the building. The optimum tank location is defined as the building height at which the annual energy generation from the turbine-generator assembly is maximized. Figure 2-3 shows that the annual energy generation is greatest when the wastewater collection tank is located on the 13^{th} floor. This result is consistent with a finding from a study by Sarkar et al. in which they showed that the best single-tank location for energy generation purposes is at the midpoint of the building. The collection tank has a volume of 4 m^3 and is sized to

minimize the cost while also being large enough to accommodate the maximum daily wastewater intake without overflowing.

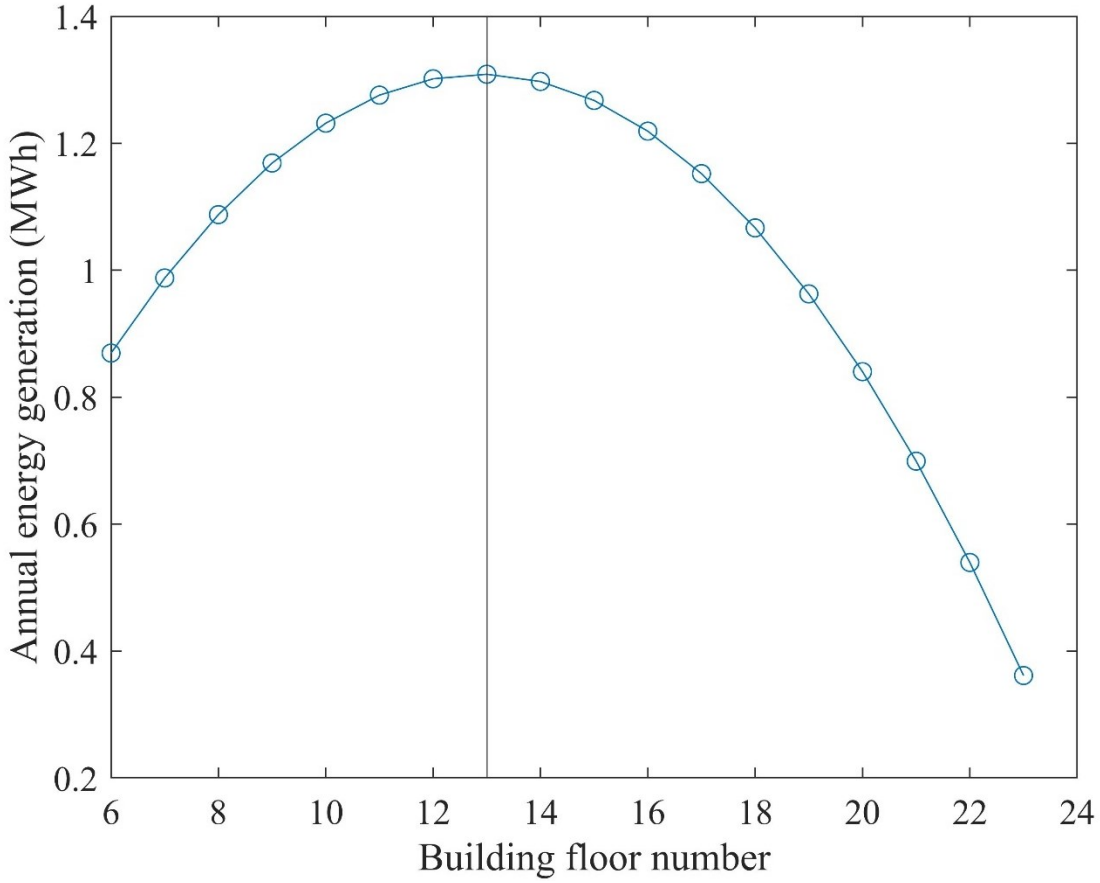

Figure 2-3: Annual energy generation from the turbine-generator assembly as a function of building floor for the case study 23-floor residential building.

2.2.3 Development of wastewater distribution

A hybrid approach consisting of measured data and an estimation technique is used to develop the wastewater distribution available for each floor and pressure zone of the case study building. The measured data provides the total daily domestic water consumption for the building as a whole over the course of a year, and is obtained from the city of Ottawa for the reference year 2019. The estimation technique is used to generate a domestic water consumption profile for each day at both the unit

level and floor level. The domestic water scheduling tool developed by Hendron and Burch is employed for this purpose [25]. The scheduling tool uses historical measured data obtained from two separate North American residential water use studies conducted on subsets of 33 homes, and 1,200 homes to output daily probabilistic water use schedules for a number of user-defined homes [26]. For example, a user can define the number of bedrooms per household, as well as the building's geographical location. The tool disaggregates hot and cold-water events for typical appliances found throughout the home such as sinks, showers, baths, clothes washers, and dishwashers, and assigns a flow rate and duration to each event. Cold water "only" events such as toilet flushes are not included in these profiles as their occurrence and duration are found to be negligible relative to mixed hot and cold-water events [26]. The scheduling tool was used to generate daily domestic water consumption profiles for each of the 249 units in the building using approximate city of Ottawa environmental conditions as inputs. These profiles were scaled to the total daily domestic water consumption value for each day of the measured reference year dataset, assuming that the total building's water usage is spread uniformly throughout the case study building. Daily floor level and pressure zone level domestic water consumption profiles were then generated by aggregating the unit distributions accordingly. The aggregated daily domestic water consumption profiles representing Floors 12-23 (*i.e.,* pressure zones 2 and 3), and Floors 6-11 (*i.e.,* pressure zone 1) of the case study building on January 1st, 2019 are shown in Figure 2-4. The temporal offset between the two profiles is mainly a

result of the random nature of the consumption events generated by the scheduling tool as well as the different number of units included in each profile.

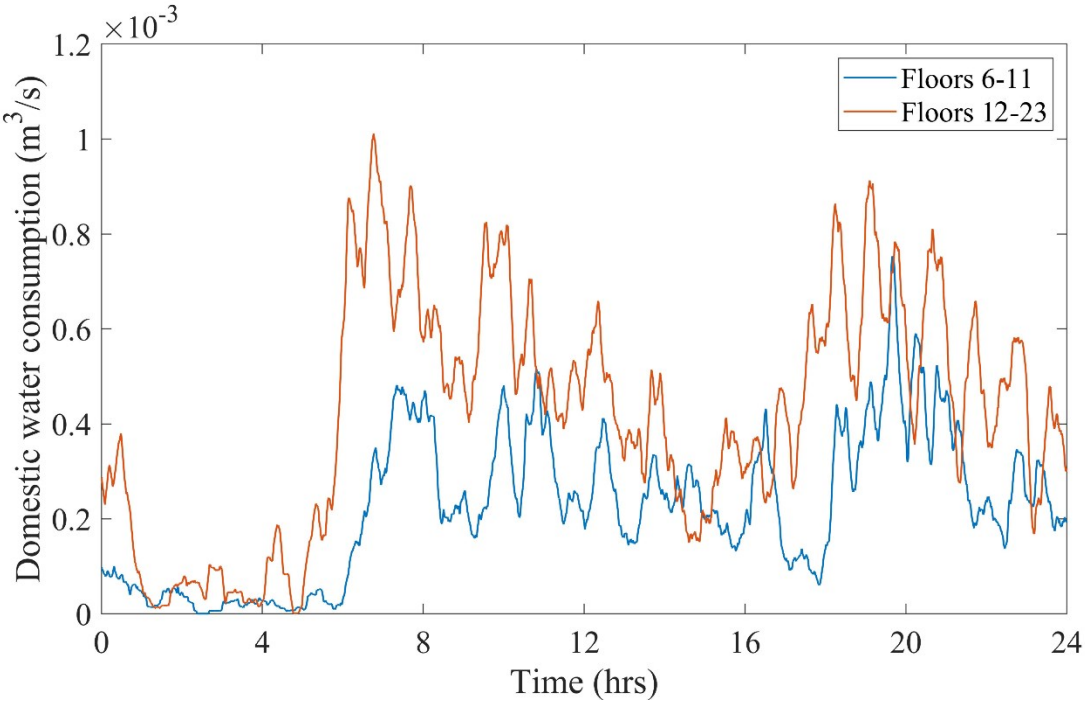

Figure 2-4: Aggregated daily domestic water consumption profiles representing Floors 12-23 and Floors 6-11 of the case study building on January 1st, 2019

2.2.4 Model dispatch strategy

A dispatch strategy (shown in Figure 2-5) is developed to simulate the operation of the wastewater hydroelectric system model over the course of a year and calculate both the pumping energy requirement, $E_{pump}(t)$, and the turbine energy generation, $E_{turbine}(t)$. The Matlab/Simscape™ tool is used to conduct the simulation using a fixed step continuous solver based on Euler's method [27]. A time step of 1 second is used in the analysis. Figure 2-5 shows that a number of fixed and variable model inputs are loaded at the start of the simulation. Fixed inputs represent technical parameters that remain constant as the simulation proceeds, whereas variable inputs represent parameters that change as a

function of time as the simulation proceeds. These inputs and their values are listed in Table 2-1.

Table 2-1: Input parameters used in wastewater hydroelectric system model dispatch strategy

Description	Symbol	Type	Value
Efficiency of turbine-generator assembly	$\eta_{turbine}$	Fixed	90%*
Efficiency of pump	η_{pump}	Fixed	82%*
Gravity	g	Fixed	9.81 m/s^2
Pipe roughness (galvanized steel)	e	Fixed	0.00015 m
Dynamic viscosity of water	μ_{water}	Fixed	0.00143 Ns/m^2
Density of water	ρ_{water}	Fixed	997 kg/m^3
Height of pressure zone 1	Δz_{PZ1}	Fixed	32 m
Height of pressure zone 2	Δz_{PZ2}	Fixed	18 m
Height of pressure zone 3	Δz_{PZ3}	Fixed	20 m
Pipe diameter below collection tank	$d_{tank_{out}}$	Fixed	0.15 m
Pipe diameter supplying water to pressure zone 1	$d_{pump_{PZ1}}$	Fixed	0.15 m
Pipe diameter supplying water to pressure zone 2	$d_{pump_{PZ2}}$	Fixed	0.13 m
Pipe diameter supplying water to pressure zone 3	$d_{pump_{PZ3}}$	Fixed	0.1 m
Mass flow rate of water entering building	$\dot{m}_{pump_{in}}(t)$	Variable	
Mass flow rate of effluent entering collection tank	$\dot{m}_{tank_{in}}(t)$	Variable	
Mass flow rate of effluent leaving collection tank	$\dot{m}_{tank_{out}}(t)$	Variable	
Velocity of effluent leaving collection tank	$u_{tank_{out}}(t)$	Variable	
Velocity of water being pumped in pressure zone 1	$u_{pump_{PZ1}}(t)$	Variable	
Velocity of water being pumped in pressure zone 2	$u_{pump_{PZ2}}(t)$	Variable	
Velocity of water being pumped in pressure zone 3	$u_{pump_{PZ3}}(t)$	Variable	

Volume of effluent in collection tank	$V_{tank}(t)$	Variable

*(Zhang & Zhang, 2014)

Once the model inputs are loaded, the dispatch strategy begins (at the first time step) by checking whether or not there is a demand for domestic water. If there is no demand, $E_{pump}(t)$ is equal to zero. If there is a demand, the pumping energy requirement, $E_{pump}(t)$, is calculated as the product of the pumping power requirement, $\dot{W}_{pump}(t)$, and the time step, Δt, as follows:

$$E_{pump}(t) = \dot{W}_{pump}(t) \times \Delta t \tag{2.1}$$

where

$$\dot{W}_{pump}(t) = \frac{\dot{m}_{pump_{in}}(t) g \Delta H_{pump}(t)}{\eta_{pump}}. \tag{2.2}$$

The term $\Delta H_{pump}(t)$ in Equation 2.2 represents the total head loss in all three pressure zones and is expressed as

$$\Delta H_{pump}(t) = \Delta H_{pump_{PZ_1}}(t) + \Delta H_{pump_{PZ_2}}(t) + \Delta H_{pump_{PZ_3}}(t). \tag{2.3}$$

The first term in Equation 2.3 represents the head loss in pressure zone 1 and is given by

$$\Delta H_{pump_{PZ_1}}(t) = \Delta z_{PZ1} \left[1 + \frac{f_{pump_{PZ_1}}(t) u_{pump_{PZ_1}}(t)^2}{2g d_{pump_{PZ_1}}}\right] \tag{2.4}$$

where the friction factor is calculated using the Chen equation [28] as follows:

$$f_{pump_{PZ_1}}(t) = \left[-2\log\left(\frac{e}{3.7065 d_{pump_{PZ_1}}} - \frac{5.0452}{Re_{pump_{PZ_1}}(t)}\log\left(\frac{1}{2.8257}\left(\frac{e}{d_{pump_{PZ_1}}}\right)^{1.1098} + \frac{5.8506}{Re_{pump_{PZ_1}}(t)^{0.8981}}\right)\right)\right]^{-2} \quad (2.5)$$

The term $Re_{pump_{PZ_1}}(t)$ in Equation 2.5 is the Reynolds number and is expressed as

$$Re_{pump_{PZ_1}}(t) = \frac{\rho_{water} u_{pump_{PZ_1}}(t) d_{pump_{PZ_1}}}{\mu_{water}}. \quad (2.6)$$

Equations 2.4-2.6 are also used to calculate the second and third terms of Equation 2.3, with the exception that the parameters are substituted with those corresponding to pressure zones 2 and 3, respectively.

Further to checking the domestic water demand, the dispatch strategy determines whether the control valve is open or closed. If it is open, and the collection tank is empty, the control valve is closed and $E_{turbine}(t)$ is equal to zero. If the control valve is open, and the collection tank is not empty, the turbine energy generation, $E_{turbine}(t)$, is calculated as the product of the turbine power output, $\dot{W}_{turbine}(t)$, and the time step, Δt, as follows:

$$E_{turbine}(t) = \dot{W}_{turbine}(t) \times \Delta t \quad (2.7)$$

where

$$\dot{W}_{turbine}(t) = \dot{m}_{tank_{out}}(t) g \Delta H_{turbine}(t) \eta_{turbine}. \quad (2.8)$$

The term $\Delta H_{turbine}(t)$ in Equation 2.8 represents the total head loss in the stack from the collection tank to the turbine and is expressed as

$$\Delta H_{turbine}(t) = \Delta z_{PZ1}\left[1 - \frac{f_{tank_{out}}(t)u_{tank_{out}}(t)^2}{2g d_{tank_{out}}}\right] \quad (2.9)$$

where

$$f_{tank_{out}}(t) = \left[-2\log\left(\frac{e}{3.7065 d_{tank_{out}}} - \frac{5.0452}{Re_{tank_{out}}(t)} log\left(\frac{1}{2.8257}\left(\frac{e}{d_{tank_{out}}}\right)^{1.1098} + \frac{5.8506}{Re_{tank_{out}}(t)^{0.8981}}\right)\right)\right]^{-2} \quad (2.10)$$

and

$$Re_{tank_{out}}(t) = \frac{\rho_{water} u_{tank_{out}}(t) d_{tank_{out}}}{\mu_{water}}. \quad (2.11)$$

Power generation is assumed to occur as soon as the control valve is opened as the pipe joining the collection tank to the turbine is always kept full. As a result, the turbine operates at nominal capacity at all times.

If on the other hand, the control valve is closed, the dispatch strategy checks whether or not it is a weekend (points I or II, respectively in Figure 2-5). The control strategy operates differently on weekends since water consumption during these periods is generally greater due to occupants being at home and not at work.

I) If it is a weekend, and the volume of effluent in the collection tank is greater than 2 m^3, the control valve is opened and $E_{turbine}(t)$ is calculated using Equation 2.7. If the volume of effluent in the collection tank is less than or equal to 2 m^3, the control valve is closed and $E_{turbine}(t)$ is equal to zero.

II) Similarly, if it is a weekday, and the volume of effluent in the collection tank is greater than 3.9 m^3, the control valve is opened and $E_{turbine}(t)$ is calculated using

Equation 2.7. If the volume of effluent in the collection tank is less than or equal to 3.9 m^3, the control valve is closed and $E_{turbine}(t)$ is equal to zero.

After each time step, model outputs (*i.e.,* $E_{pump}(t)$ and $E_{turbine}(t)$) are saved and the simulation proceeds to the next time step. After the final time step, the simulation ends.

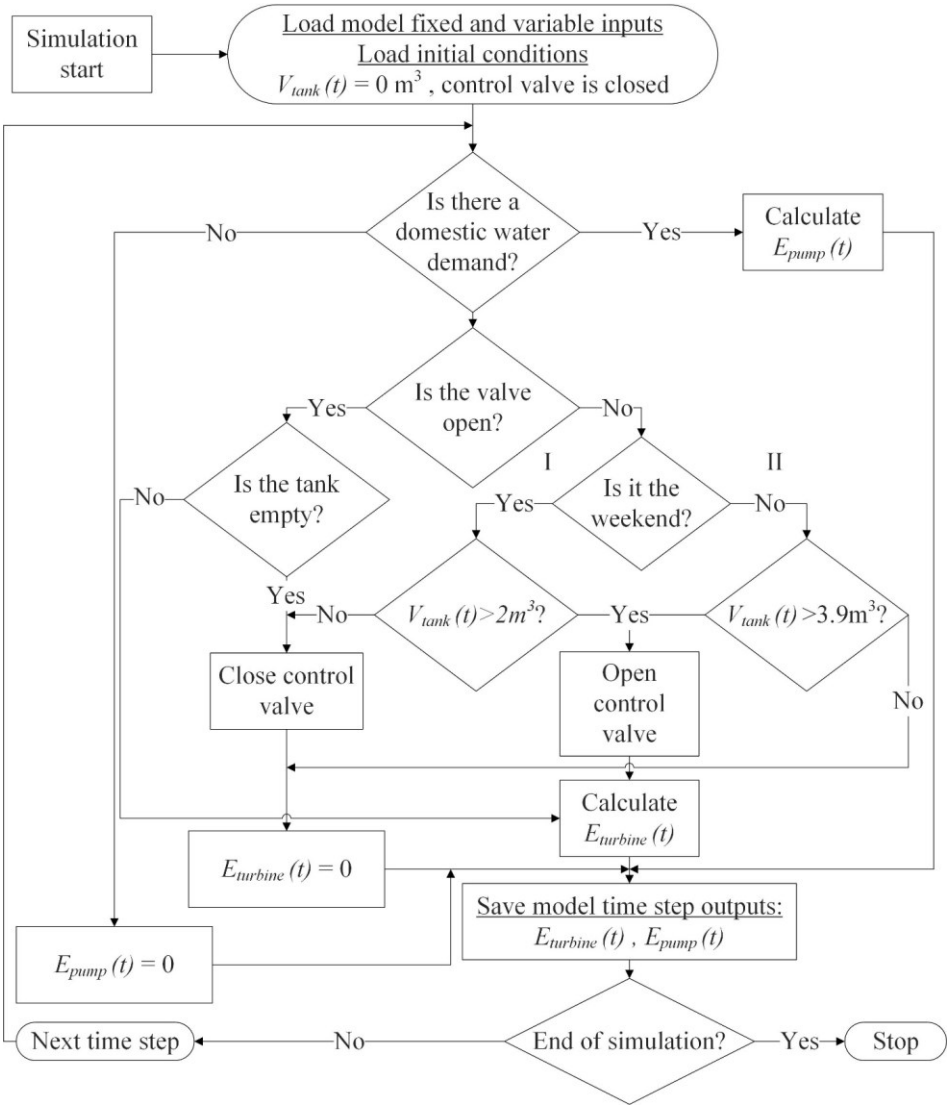

Figure 2-5: Dispatch strategy used to calculate both the pumping energy requirement, $E_{pump}(t)$, and the turbine energy generation, $E_{turbine}(t)$ over the course of a year.

2.2.5 Model Validation

The numerical model of the wastewater hydroelectric system is validated using a first principles approach that involves conducting mass and energy balance checks at every time step using the model's spatial and temporal outputs. The validation is conducted by breaking down the full system into several subcomponents (*e.g.,* turbine, pump, collection tank, pipes, etc…) and developing an equivalent Excel spreadsheet model for each of these components separately. Excel model outputs are calculated at various time steps over a range of input parameters and compared with the outputs obtained using the Simscape model. Since the maximum calculated % difference is below 2% for all cases (primarily due to rounding and approximation errors), it is assumed that mass and energy conservation is maintained in the model, and the model is performing as expected.

2.2.6 Economic model

An economic analysis is conducted on the wastewater hydroelectric system using the net present value, NPV, as a performance indicator. The net present value is a financial metric that is used to calculate the present worth of a future series of cash flows, and is given by

$$NPV = -C_c + \sum_j^k \frac{R_j - c_j}{(1+i)^j} \tag{2.12}$$

where C_c represents the system capital cost (in \$), and R_j and c_j represent the annual turbine energy revenue (in \$/yr) and the annual operations and maintenance (O&M) cost (in \$/yr), respectively.

The system capital cost includes the installed costs of both the turbine-generator assembly and collection tank. Fixed costs for additional piping are not considered in the

analysis, and it is assumed that the equipment has no salvage value at the end of its lifetime. The annual O&M cost includes annual turbine – generator assembly maintenance and collection tank cleaning. Details regarding component capacities, costs, and lifetimes are shown in Table 2-2.

Table 2-2: Wastewater hydroelectric system component capacities, costs, and lifetimes used in case study building model.

Component	Capacity	Cost	O&M cost	Lifetime
Turbine- generator assembly	300 W	993 $[1]	33.9 $[2]	50 years [3]
Collection tank	4 m^3	5,615 $[4]	286 $[5]	50 years[6]

[1] Obtained from [29]
[2] Incurred each year [30]
[3] Obtained from [31]
[4] Obatined from [32]
[5] Incurred every 4 years [33,34]
[6] Obtained from [17]

The annual turbine energy revenue is expressed as

$$R_j = r_{elec} \sum E_{turbine}(t) \tag{2.13}$$

where r_{elec} is the median electricity value in the province of Ontario (equivalent to 0.128 $/kWh [35]) and $\sum E_{turbine}(t)$ is the total amount of energy generated by the turbine on an annual basis (in kWh). All electricity generated is assumed to be sold to the grid at a value equivalent to r_{elec}. The terms i, j, and k in Equation 2.12 represent the discount rate (assumed to be 6% in the current study [36]), year, and project lifetime, respectively. A project lifetime of 50 years is used in the analysis as this is the minimum equivalent lifetime when considering all component costs.

2.2.7 Sensitivity analysis

The net present value of the proposed wastewater hydroelectric system can vary significantly based on the value of the input parameters assumed in the economic analysis. As these parameters may vary in time due to impacts such as material/energy price volatility and/or inflation, a sensitivity analysis is conducted in the current study by varying a number of key parameters presented in Section 2.2.6. These parameters are the system capital cost, the annual O&M cost, the discount rate, and the electricity rate. The following rational was used to determine upper and lower range values for these parameters. The O&M cost and discount rate are varied by plus or minus 20%, and roughly plus or minus 35% relative to the base case value, respectively, as these ranges are commonly employed in the literature when gauging the sensitivity of projects [37–40]. The system capital cost is varied based on low and high cost values (*i.e.,* $795 and $1,192, respectively) employed in a study by Basar et al. for the turbine-generator assembly, combined with a range of plus or minus 20% (relative to the base case value) for the collection tank [29]. The electricity rate is varied based on the minimum and maximum electricity rates encountered across most major cities in North America (0.073 $/kWh and 0.37 $/kWh, respectively) [41]. A best and worst-case scenario is also considered which consists of combining the upper and lower-range values for all parameters simultaneously so as to obtain the highest and lowest net present value, respectively.

2.2.8 Impacts due to building size

The net present value of the proposed system can also vary considerably with building size (*i.e.* as the number of floors, and corresponding number of units per floor increases) since there is a potential for greater amounts of energy to be generated at minimal additional cost. To determine this variation, the annual energy generation is

calculated for a number of building models (2,400 in total) that contain between 15 and 75 floors, with 10 to 50 units per floor. An upper limit of 75 floors is chosen as this number corresponds to the tallest building encountered in Canada's most populous city – Toronto [42]. The upper limit of 50 units per floor reflects an assumption made in a study by Sarkar et al. in which each building floor houses 100 residents with an average of 2 residents per unit [13]. Identical assumptions to those presented in Sections 2.2.2-2.2.7 are used to develop, simulate, and assess the techno-economic performance of the above-mentioned building models. The only exceptions involve the relative heights of the three pressure zones which are scaled linearly with building size based on a fixed ratio obtained from the case study building, and the equipment capacities (*i.e.,* pumping system, turbine-generator assembly, and collection tank) which are also scaled linearly with building size based on the total aggregated daily domestic water consumption relative to the case study building. Moreover, changes in pipe friction losses as a function of building size are not included as these are assumed to be negligible.

2.3 Results and Discussion

The following section provides an overview of the key findings of the current study. The energy generation potential of the case study building is presented initially, and is followed by a discussion on the economic performance of the proposed system as a function of a number of parameters. Several insights are drawn from the analysis which can be used to guide the design, inform policy decisions, and direct future research into building-based wastewater hydroelectric systems. These insights are described as follows:

Insight 1: *Implementing a building-based wastewater hydroelectric system can offset the total annual pumping energy requirement by up to 36% regardless of the building's height.*

Figure 2-6 shows the estimated pumping power requirement (to supply domestic water to floors 13-23) and turbine power generation for the case study building on January 1st, 2019. Based on the control algorithm described in Section 2.2.4, the turbine activates at 7 hrs when the collection tank is full, and generates power for approximately 4.5 hours until the tank is empty. A similar process occurs again from 13 hrs to 15 hrs, and 17.5 hrs to 22 hrs. The power decreases slightly during generation as the tank level and corresponding head decreases during this period. The shorter generation period beginning at 13 hrs is a result of there being reduced water consumption by building residents during this period which causes the tank to be refilled at a much lower rate. Integrating the area under each curve provides the daily pumping energy requirement and turbine energy generation.

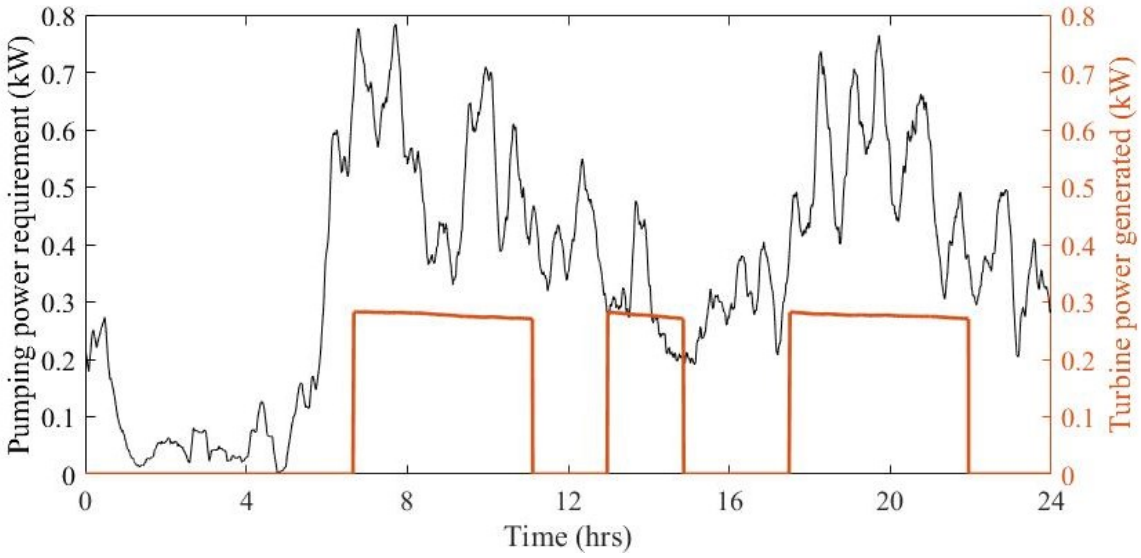

Figure 2-6: Estimated pumping power requirement and turbine energy generation for case study building on January 1st, 2019.

Table 2-3 summarizes the above-mentioned values calculated on an annual basis as well as the annual proportion of pumping energy that is offset by the turbine-generator assembly. The wastewater hydroelectric system generates 1,308 kWh annually and is capable of offsetting approximately 36% of the annual pumping energy requirement. Although the quantity of energy that is offset is negligible compared to the total annual energy requirement of any given building [43], the proposed system offers an alternative avenue for increasing building energy efficiency along with other measures such as switching to low energy lighting systems. In practice, these offsets can be implemented in any given building in any location so long as an appropriate power crediting mechanism such as net metering is available through the local power utility. Net metering allows surplus power from generators to be transferred to the utility power grid, allowing consumers to offset the cost of power drawn at different times of the day from the grid [44]. In the province of Ontario, renewably sourced generators that are below 10 kW of capacity are currently eligible to enter into a net metering contract with the power utility [45]. The contract allows for energy storage to be paired with the renewable energy source, and excess generation credits can be brought forward for up to one year to be used to offset future electricity costs.

Table 2-3: Annual estimated pumping energy requirement and turbine energy generation for case study building for the reference year.

Component	Annual energy requirement (kWh)	Annual energy generation (kWh)	Proportion of annual energy requirement (%)
Pumping system	3,560	0	100
Turbine-generator assembly	0	1,308	36

Results from other building models (see Section 2.2.8) show that the offset value of 36% remains approximately constant (with an error of $\pm$ 2%) regardless of building size. The reason this value does not deviate is due to the fact that wastewater first needs to be pumped up from ground-level (as domestic water) to a given elevation before it can drain back down via gravity to the turbine-generator assembly to be used for power generation purposes. The ratio of the pumping head (*i.e.,* the head difference between the pumping system and the water fixtures at elevation) to turbine head (*i.e.,* the head difference between the collection tank and the turbine-generator assembly) in this process is independent of building height.

Insight 2: *Increasing the electricity rate has the single largest positive impact on the cost-effectiveness of the wastewater hydroelectric system for a building of a given size.*

A net present value of -$5,479 is found for the case study building wastewater hydroelectric system, which indicates that the selected building is not an ideal host from a cost-effectiveness standpoint. Figure 2-7 shows the sensitivity of the case study system's NPV as a function of a number of upper and lower range parameter values. Although the NPV for the case study building remains negative across all parameter ranges shown, it is of interest to see which parameters have a greater or lesser impact on the NPV of the system. Aside from the best/worst case scenario which demonstrates the maximum and minimum variation in NPV attainable, an increase in the electricity rate has the next single greatest impact on NPV (*i.e.,* it causes it to nearly double). Similarly, decreasing the capital cost causes an increase in NPV of roughly 25%, whereas decreasing the discount rate, and

the annual O&M cost correspond to much smaller NPV increases of approximately 11% and 8%, respectively.

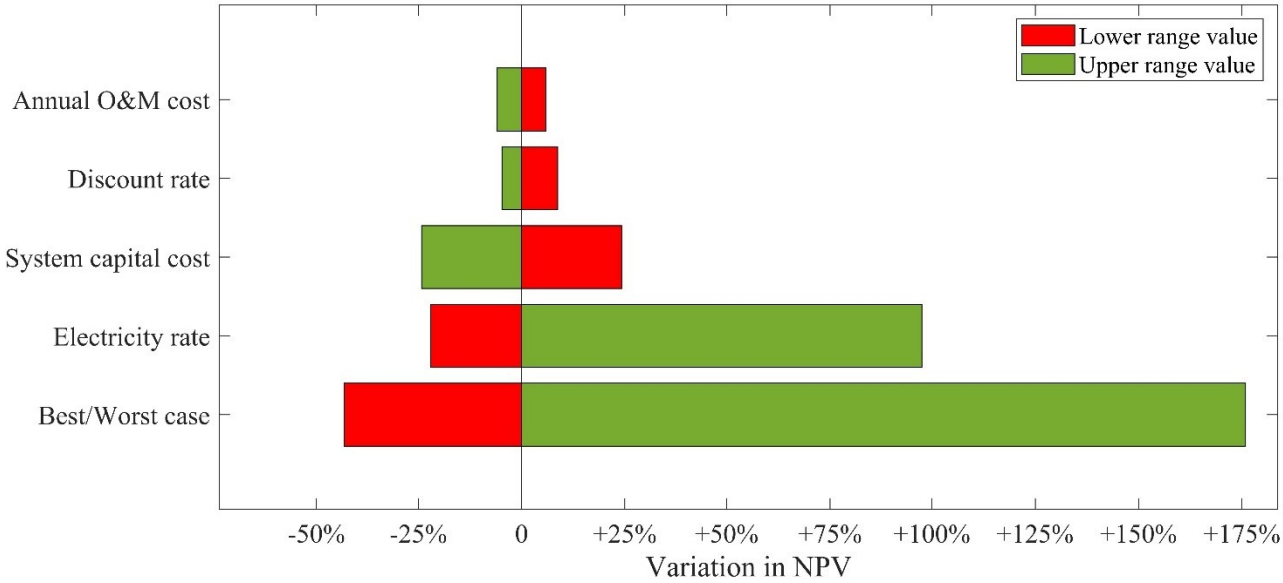

Figure 2-7: Sensitivity of net present value (NPV) of case study building wastewater hydroelectric system from varying a number of economic parameters from base case values to lower and upper range values.

The finding that the NPV increases as a function of electricity rate shows that these systems are well suited for North American jurisdictions in which grid power generation costs are high. Examples of such jurisdictions include American cities like San Francisco, Boston, and New York, that in 2020 had average residential electricity prices of 0.37 $/kWh, 0.34 $/kWh, and 0.33 $/kWh, respectively [41]. In fact, if the Ottawa case study building were to operate using the same electricity rate as that of San Francisco, then the system NPV would approximately break even, which shows that at these higher rates even smaller building systems can be cost effective.

This finding also brings to light the possibility that further economic improvements are possible when changes are made to the way in which the system operates. These changes are most applicable to buildings that are located in areas where grid demand

response programs like time of use (TOU) pricing are available. TOU pricing is a utility rate plan that most commonly applies to residential customers in which electricity rates vary depending on the time of day, season, and day type (*i.e.*, either a weekday, weekend, or holiday) [46]. For example, as of June 2021 in the province of Ontario, a TOU pricing program has been put into effect which comprises three different electricity rates corresponding to off-peak (0.082 $/kWh), mid-peak (0.113 $/kWh), and on-peak (0.17 $/kWh) periods (Hydro Ottawa, 2021b). In contrast, the state of California currently uses a TOU pricing program that consits of a two tier rate structure in which on-peak and off peak rates are equivalent to 0.28 $/kWh and 0.38 $/kWh, respectively [47]. Therefore, rather than wait for the collection tank to fill to a prespecified volume before generating power (as depicted by the dispatch strategy shown in Figure 2-5), the system could in theory shift generation to peak load periods in order to maximize daily revenue from electricity sales. Alternatively, a building could supply a portion of its own electricity load during peak load periods, thereby avoiding the need to purchase electricity at a higher rate.

Insight 3: *Both the annual energy generation and system cost-effectiveness increase as the building size increases.*

Figure 2-8 demonstrates via a surface plot the impacts of varying the building size on the proposed system's annual energy generation and cost-effectiveness. In total, 2,400 building models are assessed corresponding to buildings that contain between 15 and 75 floors, with 10 to 50 units per floor. The case study building is shown in the figure for comparison. The red regions of the surface plot indicate building sizes that are infeasible from a cost perspective (*i.e.,* the NPV<0), whereas the blue regions indicate building sizes

that are cost-effective (*i.e.,* the NPV>0) and thus worthy of consideration for implementation. For instance, a system installed in a tall building that has 70 floors and 20 units per floor can generate approximately 16,463 kWh annually and provide a positive NPV of $8,793. Similarly, a system installed in a shorter building that has 45 floors and 45 units per floor can generate roughly 15,232 kWh annually and also provide a positive NPV of $5,378. Buildings with 74 floors and 7 units per floor, on the other hand, have an NPV roughly equal to zero, and the same can be said on the opposite end of the spectrum for buildings with 35 floors and 47 units per floor. These cases in the order given are considered to be the breakeven scenarios as the number of floors per building and the number of units per floor increase, respectively. Overall, the greater the building size is, the more potential there exists for energy generation (mainly due to the additional available flow and/or higher head differential), and the more cost-effective the system becomes. It should be noted, however, that Figure 2-8 is generated using the base case assumptions presented in Sections 2.2.2-2.2.7, therefore, changes from these assumptions could in certain instances lead to smaller building systems also being cost-effective.

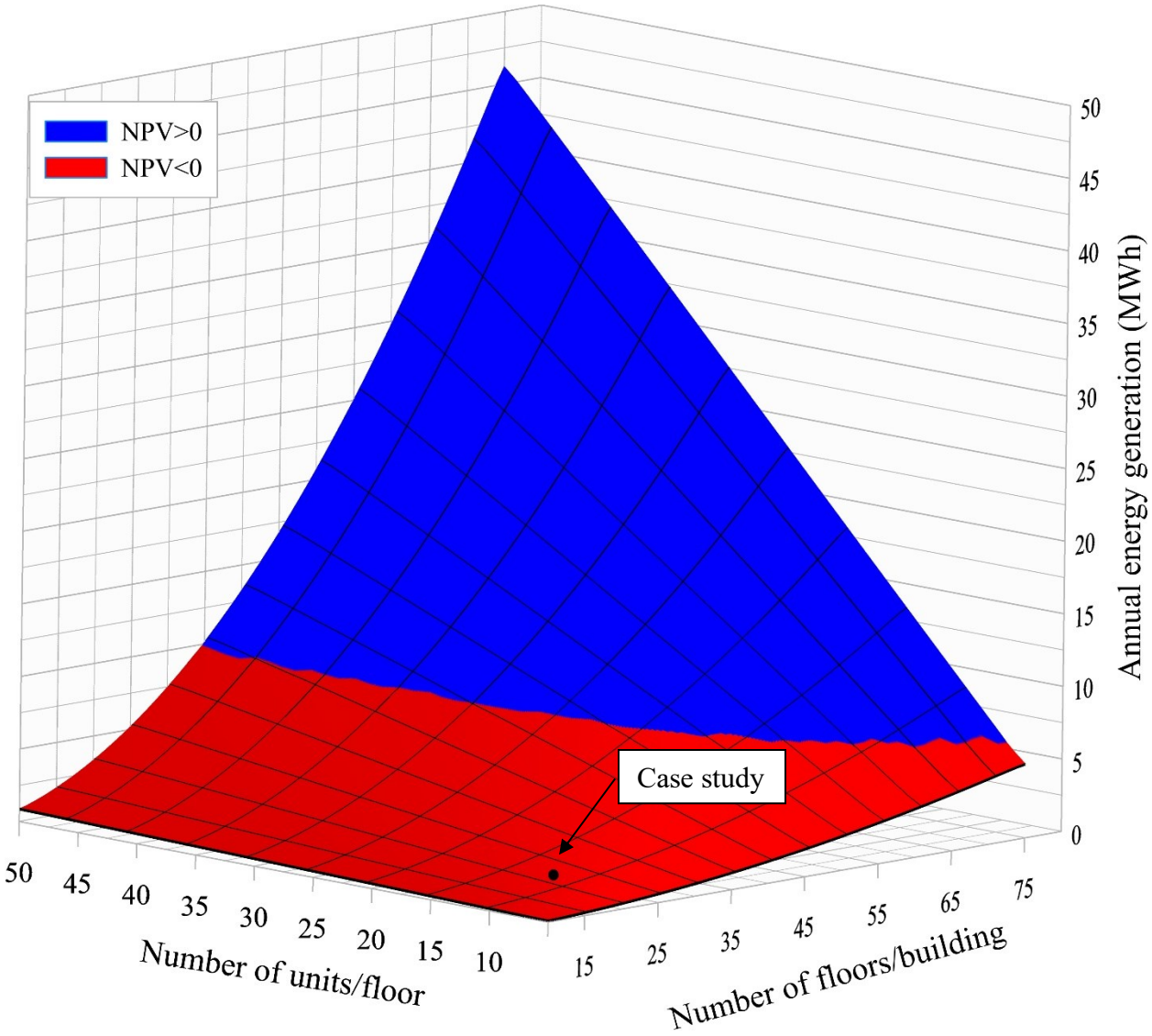

Figure 2-8: Annual energy generation as a function of the number of floors in a building and the number of units per floor based on an analysis of 2,400 building models. The blue region depicts building sizes that are cost effective (*i.e.*, the NPV>0).

Insight 4: *Incorporating the proposed wastewater hydroelectric system in new buildings can provide significant local energy generation potential as major cities worldwide continue to densify and expand upwards.*

Figure 2-9 shows the average number of floors of the 100 tallest buildings in three World cities known to have the most skyscrapers (*i.e.,* buildings with heights exceeding 150 m) [48]: Dubai, New York, and Hong Kong ; and three major Canadian cities: Toronto, Vancouver, and Ottawa; for comparison. The first three cities in the order given have an average of 62, 60, and 59 floors, respectively, whereas the three Canadian cities have an average of 47, 33, and 21 floors, respectively. The buildings shown include a mixture of residential, commercial, and institutional sector buildings. Although the average building height in the Canadian cities is lower, this trend is expected to change in the coming decades. From 1950 to 2015 the percentage of North Americans living in urban areas increased from 64% to 82%, while the population itself doubled. It is expected that this stated percentage will increase to 87% as the population continues to grow from 365 to 435 million by 2050 [49]. To accommodate for this increase in population in centralized areas and avoid urban sprawl, cities will need to densify and expand upwards, resulting in new buildings being built [50]. Other major global cities like Singapore and Shanghai currently have plans in place to build taller buildings as a solution to land scarcity [51, 52].

Incorporating the proposed wastewater hydroelectric system in these buildings during construction can provide building owners with a valuable energy generation resource, and also potentially provide a number of advantages from a planning, design, and cost-effectiveness standpoint. For example, standard wastewater hydroelectric system designs can be conceived and optimized for a particular building type prior to construction. Retrofitting existing buildings, on the other hand, can be challenging and expensive as there is currently no standard piping layout for building wastewater systems in North America, and as such every building requires a unique custom system design [53].

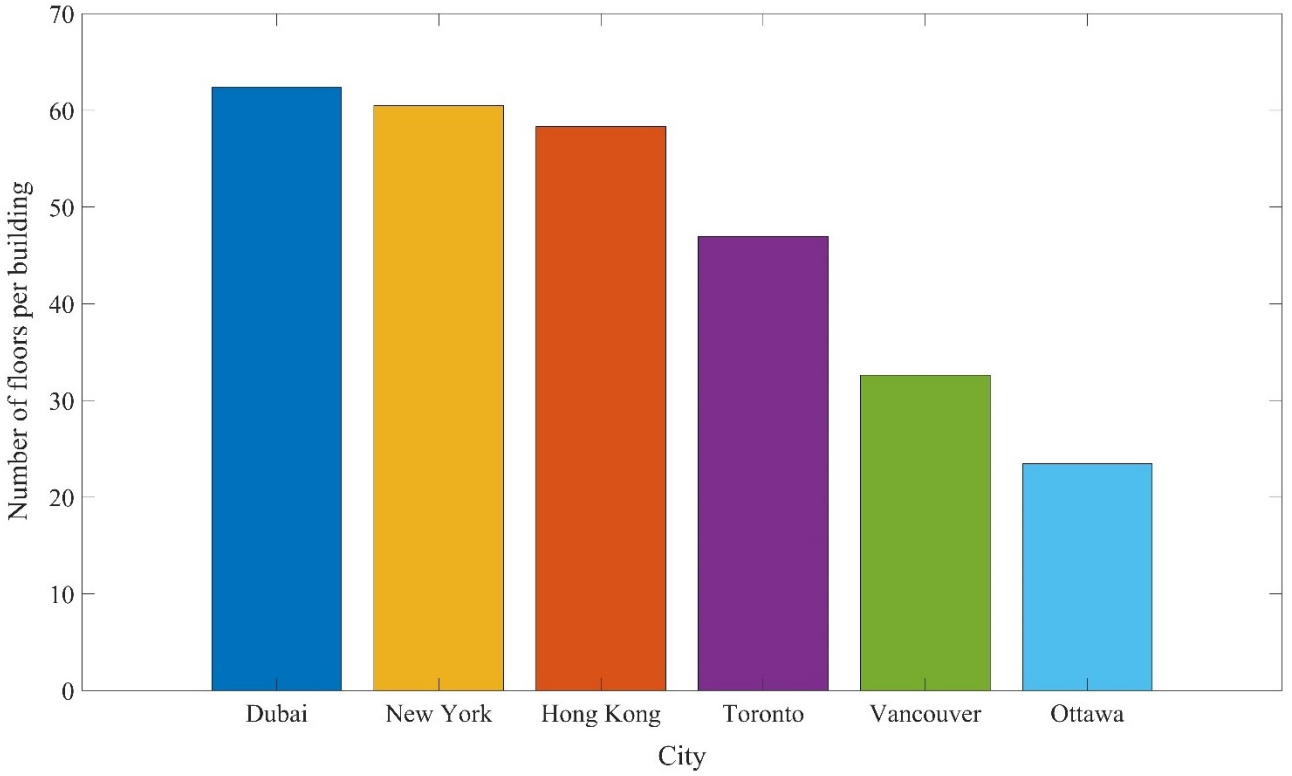

Figure 2-9: Average number of floors of 100 tallest buildings in three World cities known to have the most skyscrapers, and three major Canadian cities for comparison.

When installed in multiple buildings as part of a distributed generation network, these systems can also present potential advantages to the local electrical grid operator such as providing additional low-carbon and cost-effective short-term energy storage capacity and an alternative means of increasing overall grid stability [54].

2.3.1 Limitations of study and recommendations for future work

In the current study, a wastewater hydroelectric system has been proposed for generating electricity in tall buildings. Although the study's findings are promising, especially for systems installed in buildings of a given size across multiple city locations, they are limited in that they are based on the following simplifying assumptions:

- Wastewater held in the collection tank and flowing through the turbine is assumed to be pure water. Therefore, no consideration is given to the treatment of potential

solids contained in the effluent stream. In practice, this issue may be addressed via the implementation of a wastewater macerating system installed in the collection tank similar to those used in self contained wastewater treatment plants [55], or bioprocessing plants [56]. Macerating systems would need to be placed upstream of the mechanical equipment and use a combination of screens and grinders to minimize solid particles in the fluid stream [57]. Large particles would be removed from the system by allowing them to flow into the effluent pipe that is connected to the units located below the collection tank. Another issue that needs to be investigated is the impact of effluent wastewater fouling on system performance. This problem is commonly encountered in wastewater heat exchangers and is typically addressed via the use of inhibitors, ultrasonic devices, or nonoxidizing biocides [58]. Although the techniques stated above may be used to address these issues, it is likely that their inclusion in the proposed system will further decrease the system's cost effectiveness.

- Building codes and regulations have not been considered as these are likely to change from one jurisdiction to another. Of particular importance is the issue of placing a wastewater collection tank indoors. Similarly, research is needed to determine the impact of discharging wastewater collection tanks from multiple buildings on the local surrounding sewer system.
- The economic analysis is based on the system operating under a utility-level net metering program. Net metering is highly jurisdiction dependent therefore is not available in all cities [59].

- No consideration is given to the value of the building floor area that is taken up by the proposed system in the economic analysis. This space could otherwise be rented or leased by the building owner as a means to provide additional revenue, therefore, including it in the analysis would likely decrease the system's cost effectiveness.

Potential recommendations for future work regarding the proposed wastewater hydroelectric system include:

- Investigating the use of alternative system configurations comprising multiple tanks and turbines on different floors,
- Determining the impact of varying the size of the collection tank(s),
- Assessing the potential benefits of separating greywater and blackwater sources, and
- Optimizing the system's control. For example, it may be advantageous to include a temporal parameter in the dispatch strategy that allows the system to generate power during peak electricity rate periods, thereby improving the economic performance of the system.

2.4 Conclusion

A numerical model has been developed in the Matlab/Simscape™ environment to simulate and assess the potential techno-economic benefits of incorporating a wastewater hydroelectric system in buildings of varying size. Data from an existing building located in Ottawa, Canada was used to formulate the base case in the study. 2,400 additional model scenarios were considered that correspond to buildings that contain between 15 and 75 floors, with 10 to 50 units per floor. A number of technical parameters were calculated for

each building scenario such as the annual pumping energy requirement and the annual turbine energy generation, as well as the net present value of the wastewater hydroelectric system over its operational lifetime. A sensitivity analysis was also conducted to determine the impact of varying different parameters on the net present value of the system. The following key insights were obtained:

- Implementing a building-based wastewater hydroelectric system can offset the total annual pumping energy requirement by up to 36% regardless of the building's height.
- Increasing the electricity rate has the single largest positive impact on the cost-effectiveness of the wastewater hydroelectric system for a building of a given size.
- Both the annual energy generation and system cost-effectiveness increase as the building size increases. Under Ontario's average electricity rate, the financial breakeven point occurs in buildings that have a minimum of 35 floors with at least 47 units per floor. Conversely, under a higher average electricity rate such as that encountered in California, this breakeven point occurs in smaller buildings.
- Incorporating the proposed wastewater hydroelectric system in new buildings worldwide can provide significant local energy generation potential as major cities continue to densify and expand upwards.

The current study has shown that there is value in the potential energy available in a building's wastewater, and this value will likely increase as society's energy demands continue to grow. However, these results are limited to individual buildings, and analyzing these systems on a city-wide scale would require an expanded study that takes into account impacts on the electricity grid.

Chapter 3

This chapter has been submitted for publication as:

T. Walker, and J. Duquette, (2021) “Evaluation of building-based hydroelectric systems as a rapidly deployable grid-scale energy storage solution,” *Journal of Energy Storage* [Under Review].

Chapter 3: Evaluation of building-based hydroelectric systems as a rapidly deployable grid-scale energy storage solution

3.1 Introduction

In order to address the objectives outlined in Chapter 1, numerical models corresponding to a typical BBGM and BBPH system are constructed using the Matlab^{TM} mathematical programming tool, and time series simulations are conducted for buildings ranging in height from 50 m to 300 m. Three additional configurations are considered for the BBGM system that include two, three, and four columns per building. To gauge the impact of varying a number of critical system parameters, a sensitivity analysis is also conducted on the BBGM system. Finally, a performance comparison is made between the above-mentioned technologies and the following two conventional technologies: NGPPs, and LIBPs. The performance of each system is quantified by calculating the variable storage cost (in $/kWh), and the levelized electricity cost (LEC) (also in $/kWh).

3.2 Methodology

The following sub-sections provide details regarding the modelling framework, scenarios, and performance metrics utilized in the current study.

3.2.1 System layout and modelling assumptions

A schematic of the BBPH and BBGM system layouts proposed in this study are shown in Figures 3-1a and 3-1b, respectively. The BBPH system is composed of a pump and turbine assembly, a lower reservoir, an upper reservoir, and a penstock that connects the two reservoirs. The volume of each reservoir is 32.6 m^3 which corresponds to the

volume of a standard rooftop swimming pool. This volume is considered to be a conservative upper limit in the current study to ensure that the loading requirements on the building's roof are not exceeded [60]. There are currently no standards regarding the maximum allowable size of a roof-top water tank for a given building across multiple jurisdictions in North America.

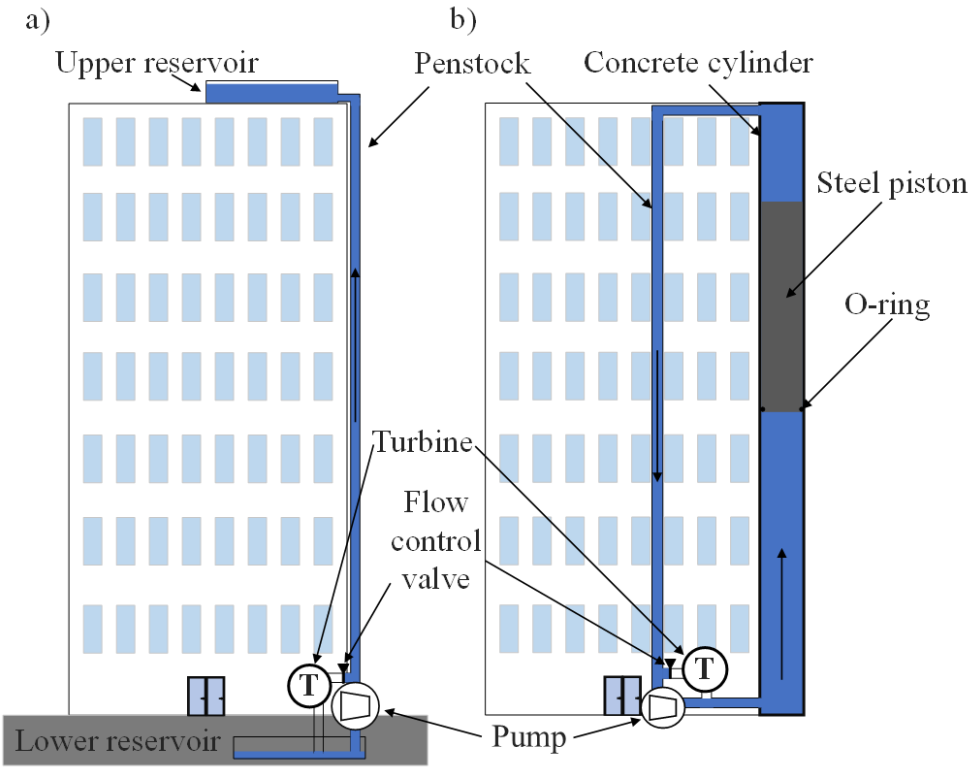

Figure 3-1: Schematic of a) building based pumped hydro (BBPH) system, and b) building based gravity module (BBGM) system in pumping mode.

The BBGM system comprises a pump and turbine assembly, a penstock, a concrete column, a steel piston, and a sealing O-ring that is located between the column and the piston. The column is made of concrete and spans the full height of the building. The steel piston is assumed to be delivered in several smaller cylindrical sections and assembled on-site. The steel piston diameter and height is roughly sized to be within the maximum

allowable freight volume of a conventional low-bed transport truck [61]. Details of the BBGM piston and column are shown in Table 3-1.

Table 3-1: Details of the BBGM column and piston.

Component	Diameter (m)	Height (m)	Material
Piston	2.6	13.5	Steel
Column (inner)	2.6	Equivalent to building height	Concrete

The following assumptions are taken to develop the BBPH and BBGM models:

- The working fluid is water (although a glycol mix may be needed in practice to avoid freezing).
- Minor losses from fixtures and fittings are neglected and friction losses from horizontal pipe lengths are ignored.
- A Francis-type turbine is selected due to its applicability to mid-range head and flow values such as those encountered in the proposed systems [62].
- A flow control valve is used to alternate the flow direction between the pump and the turbine depending if the system is charging or discharging.
- The pump and turbine operate at constant speed and constant efficiency. For the BBGM model, a simplified approach developed by Yokoyama et al. [63] is used to emulate friction losses that occur between the sealing O-ring and the wall of the concrete column. This approach consists of applying a 1.5% friction penalty to the net turbine efficiency, as shown in Table 3-2.

Table 3-2: Efficiency parameters of the pump and turbine used in the BBPH and BBGM models.

Component	Mechanical Efficiency (%)	Electrical efficiency (%)	Friction Penalty (%)	Net Efficiency (%)
Pump	87.5 [6]	96 [64]	-	84.0
BBGM Turbine	95 [62]	96 [64]	1.5 [6]	89.7
BBPH Turbine	95 [62]	96 [64]	-	91.2

3.2.2 Estimation of pump energy consumption

The energy (in Wh) consumed by the pump at any given timestep, Δt, is given by:

$$E_p = W_p \, \Delta t \, , \tag{3.14}$$

where W_p is the power (in W) consumed by the pump and is expressed as

$$W_p = \frac{\dot{\mathrm{m}} \, \mathrm{g} \, \Delta \mathrm{H}_p}{\eta_p}. \tag{3.15}$$

The parameters $\dot{\mathrm{m}}$, g, $\Delta \mathrm{H}_p$, and η_p in Equation 3.2 represent the mass flow rate (in kg/s), gravitational constant (in m/s^2), total head (in m), and total pump net efficiency, respectively. L is the penstock length (in m). The total head loss is determined from the modified Bernoulli equation [65]. The following relations apply to the BBPH and BBGM models, respectively:

$$\Delta \mathrm{H}_p = L + \frac{fL}{d}\frac{V^2}{2g}, \tag{3.16a}$$

$$\Delta \mathrm{H}_p = \frac{\Delta \mathrm{P}}{\rho_{water} \, g} + \frac{fL}{d}\frac{V^2}{2g}, \tag{3.3b}$$

where f is the friction factor, d is the penstock diameter (in m), V is the fluid velocity (in m/s), ρ_{water} is the density of water (in kg/m^3), and ΔP is the pressure required (in Pa) for

the pump to overcome the steel piston's weight. The latter parameter is derived by applying a force balance to the steel piston and subtracting the weight of the water displaced by the piston from the result as follows:

$$\Delta \mathrm{P} = \frac{m_{steel} g}{A} - \frac{m_{water} g}{A}, \tag{3.4}$$

where m_{steel} and m_{water} represent the mass of the steel piston (in kg) and mass of an equivalent volume of water (in kg), respectively, and A represents the area at the base of the steel piston (in m^2).

The friction factor is determined from the Chen equation [28]:

$$f = (-2\log\left(\frac{\mathrm{e}}{3.7065\mathrm{d}} - \frac{5.0452}{Re}\log\left(\frac{1}{2.8257}\left(\frac{\mathrm{e}}{\mathrm{d}}\right)^{1.1098} + \frac{5.8506}{Re^{0.8981}}\right)\right))^{-2}, \tag{3.5}$$

where e is the penstock roughness (m) and Re is the Reynolds number given by:

$$\mathbf{Re} = \frac{\boldsymbol{\rho_{water} V d}}{\boldsymbol{\mu_{water}}}. \tag{3.6}$$

The parameter μ_{water} in Equation 4.6 represents the dynamic viscosity of water (Ns/m^2), and its value is shown in Table 3-3 alongside other parameter values used in the models.

Table 3-3: Parameters used for estimating pump energy consumption.

Parameter	Values
Roughness of Steel penstock (e)	0.000046 m [66]
Dynamic Viscosity of water (μ_{water})	0.00143 Ns/m^2
Density of water (ρ_{water})	997 kg/m^3
Density of steel (ρ_s)	7,871 kg/m^3 [67]

3.2.3 Estimation of turbine energy generation

A similar set of equations to those shown in Section 3.2.2 are used to estimate the turbine energy generation. The energy (in Wh) generated by the turbine at any given timestep, Δt, is given by:

$$E_t = W_t \, \Delta t \, , \tag{3.7}$$

where W_t is the power (in W) generated by the turbine and is expressed as

$$W_t = \dot{\mathrm{m}} \, \mathrm{g} \, \Delta \mathrm{H}_t \, \eta_t . \tag{3.8}$$

The parameters η_t and $\Delta \mathrm{H}_t$ in Equation 3.8 represent the total turbine net efficiency and the total head (in m), respectively. The total head loss for the BBPH and BBGM models in the order stated can be expressed by the following relations:

$$\Delta \mathrm{H}_t = \mathrm{L} - \frac{fL}{d}\frac{V^2}{2g}, \tag{3.9a}$$

$$\Delta \mathrm{H}_t = \frac{\Delta \mathrm{P}}{\rho_w \, g} - \frac{fL}{d}\frac{V^2}{2g}. \tag{3.9b}$$

3.2.4 BBPH and BBGM scenarios

BBPH and BBGM system performance is analyzed over a number of scenarios in which the building height is made to increase from 50 m to 300 m in 1-m increments. The minimum height (*i.e,* 50 m) is chosen arbitrarily as it was found from preliminary simulations that there is little value to be gained below this threshold. The maximum height is selected as it corresponds to the maximum building height encountered in some of the world's largest skyscraper-laden cities such as Toronto, New York, Dubai, and Hong Kong [42]. For all scenarios, components are sized in order to allow the system to either charge or discharge in exactly one hour under nominal conditions (resulting in a charge/discharge cycle time, σ_{cycle}, of two hours). The sizing parameter values of the BBPH system

therefore vary according to the ranges shown in Table 3-4 across all building height scenarios.

For the BBGM system, the penstock diameter also varies in size as the building height increases as shown in Table 3-4. This is due to the significant increase in water volume in the column as the building height increases, which requires higher flow rates in the penstock. The penstock diameter in each BBGM building height scenario is therefore sized to the maximum allowable flowrate according to standard design practice [68].

Table 3-4: Range of component parameter values across BBPH and BBGM building height scenarios.

System Type	Component	Parameter	Value/Range
BBGM	Column	Volume	265-1,588 m^3
	Penstock	Length	50-300 m
		Diameter	0.203-0.406 m
	Pump	Nominal capacity	58.4-461.9 kW
	Turbine	Nominal capacity	43.9-339.5 kW
		σ_{cycle}	2 hours
BBPH	Upper/lower reservoir	Volume	32.6 m^3
	Penstock	Length	50-300 m
		Diameter	0.10 m
	Pump	Nominal capacity	5.3-31.6 kW
	Turbine	Nominal capacity	4.0-23.8 kW
		σ_{cycle}	2 hours

3.2.5 Multi-column BBGM scenarios

A number of additional BBGM scenarios are considered in the analysis since unlike BBPH systems which are limited to a single maximum reservoir volume on the roof, these

systems are modular and can be expanded to include multiple columns. Scenarios with buildings containing two, three, and four columns are investigated and the same height variations as described in Section 3.2.4 are assessed. However, unlike Section 3.2.4, the time required to charge or discharge the system under nominal conditions increases by one hour for each additional column that is added. For example, a one-column BBGM system requires one hour to discharge, whereas a four-column system requires four hours. This design consideration is implemented to maintain a constant power capacity across all multi-column BBGM scenarios, which helps to minimize the total capital system cost as the number of columns increases. A scaled rendering of the four-column BBGM system assessed in the current study (with a ground floor footprint of 2,160 m^2) is shown in Figure 3-2.

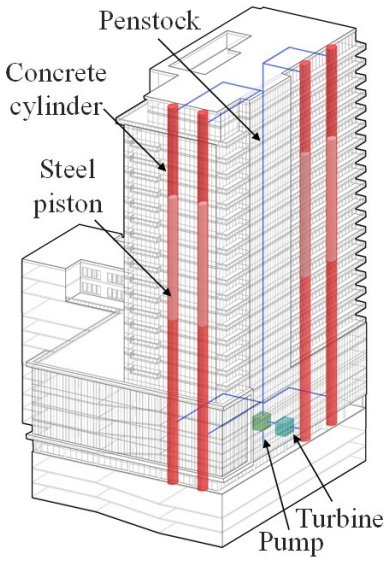

Figure 3-2: Scaled rendering of the proposed four-column BBGM system with centralized penstock [69].

Figure 3-2 depicts a simplified piping layout that comprises a single centralized penstock. The sizing parameter values of the multi-column BBGM system vary according to the ranges shown in Table 3-5 across all building height scenarios.

Table 3-5: Range of component parameter values across multi-column BBGM building height scenarios.

Number of columns	Component	Parameter	Value/Range
2	Column (total)	Volume	531- 3,175 m^3
	Centralized penstock	Length	50-300 m
		Diameter	0.203-0.406 m
	Pump	Nominal capacity	58.4-461.9 kW
	Turbine	Nominal capacity	43.9-339.5 kW
		σ_{cycle}	4 hours
3	Column (total)	Volume	796-4,762 m^3
	Centralized penstock	Length	50-300 m
		Diameter	0.203-0.406 m
	Pump	Nominal capacity	58.4-461.9 kW
	Turbine	Nominal capacity	43.9-339.5 kW
		σ_{cycle}	6 hours
4	Column (total)	Volume	1062-6,350 m^3
	Centralized penstock	Length	50-300 m
		Diameter	0.203-0.406 m
	Pump	Nominal capacity	58.4-461.9 kW
	Turbine	Nominal capacity	43.9-339.5 kW
		σ_{cycle}	8 hours

3.2.6 Scenario dispatch

Time series simulations (Matlab®) are conducted for all scenarios listed in Sections 3.2.4 and 3.2.5 using hourly time steps over the course of one year. The scenario dispatch algorithm calculates the annual turbine energy generation, $E_{t_{annual}}$, (in kWh) and the annual pumping energy consumption, $E_{p_{annual}}$, (in kWh) for each scenario assessed in the

current study, assuming that the system performs a charge/discharge cycle twice per day. These parameters can be expressed by the following relations:

$$E_{t_{annual}} = \frac{365 W_t \sigma_{cycle}}{1000}, \tag{3.10}$$

$$E_{p_{annual}} = \frac{365 W_p \sigma_{cycle}}{1000}, \tag{3.11}$$

where the integer "365" in Equations 3.10 and 3.11 represents the number of days per year.

3.2.7 Model validation

The BBPH and BBGM models developed in the current study are validated using a first principles approach that involves conducting energy, force, and pressure balance checks on the models' spatial and temporal outputs. This method ensures that energy conservation is maintained at all times and the models are performing as expected.

3.2.8 Economic model

An economic analysis is conducted on the BBGM and BBPH scenarios using the levelized electricity cost (LEC), and variable storage cost (C_{se}) as performance indicators. The LEC (in \$/kWh) is defined as the cost per unit of electricity produced in a given energy system over a year [70], and is expressed as

$$LEC = \frac{CRF\ NPC}{E_{t_{annual}}}, \tag{3.12}$$

where NPC is the net present energy system cost (in \$), CRF is the capital recovery factor, and i is the discount rate (assumed to be 8% in the current study [39]). The NPC and CRF are given by the following relations [71]:

$$NPC = C + \sum_{j}^{k} \frac{c_j}{(1+i)^j}, \tag{3.13}$$

$$CRF = \frac{i\,(1+i)^k}{(1+i)^k - 1}, \tag{3.14}$$

where j and k represent the year and project lifetime (assumed to be 50 years in the current study with an equivalent component lifetime [17]), and C and c are the total capital system cost (in $) and annual variable system cost (in $/yr), respectively. The total capital system cost is represented for a) the BBGM system, and b) the BBPH system, respectively, as

$$C = C_t + C_p + C_s + C_{pe} + C_{co} \tag{3.15a}$$

$$C = C_t + C_p + C_{pe} + 2C_r \tag{3.15b}$$

where C_t is the capital cost of the turbine assembly, C_p is the capital pump assembly cost, C_s is the capital cost of the steel piston, C_{pe} is the penstock capital cost, C_{co} is the capital cost of the concrete containment column, and C_r is the capital cost of a single reservoir (assumed to be $20,615 in the current study [32]). The latter value is multiplied by two to account for both the upper and lower reservoirs present in the BBPH system. The capital cost of the turbine assembly is determined from an equation developed by Aggidis et al. [72]:

$$C_t = 12000\left(\frac{W_t}{H^{0.2}}\right)^{0.56} \tag{3.16}$$

where H represents the equivalent gross head of water (in m) for which the turbine is designed to operate at, and W_t is given in units of kW. Equation 3.16 was developed using data from a large number of small-scale hydro plants in the UK with head values ranging

from 2 to 200 m and power capacities ranging from 25 to 900 kW, and includes turbine, gear box, generator, and other electromechanical equipment costs required to operate the system. Estimates produced using Equation 3.16 are reported to lie within ±25% of published values. The capital cost of the pump assembly is estimated using a relation developed by Wilson et al. [73]:

$$C_p = (1428\, N_s) + 50000, \tag{3.17}$$

where N_s is the specific speed of the pump and is given by

$$N_s = \omega \left(\frac{Q^{0.5}}{H^{0.75}}\right). \tag{3.18}$$

The parameters ω and Q in Equation 3.18 are the rotational speed of the pump (assumed to be 800 rpm in the current study [6]) and the flowrate (in m^3/s). The capital cost of the steel piston for the gravity module is calculated by multiplying the piston's mass (assumed to be roughly 573.4 tonnes in the current study) by the current market price of raw steel (assumed to be approximately \$931/tonne [74]). An additional 20% is added to this cost to account for the manufacturing of the piston and purchase of the O-ring. The above stated value can be seen as a conservative estimate as no specific cost data could be obtained for such a large-diameter steel cylinder. The capital costs of the penstock (made of Schedule 40 steel pipe) and the concrete gravity module column are determined on a per length basis from the RSMeans database [32], and are estimated to be \$335-\$848.7/m and \$2,965/m, respectively. The range associated with the penstock cost is due to the varying penstock diameter as a function of building height (see Tables 3-4 and 3-5). These costs include allowances for labour, installation, and supporting materials. The annual variable system cost (for both BBGM and BBPH) is represented as

$$c = c_t + c_p \,, \tag{3.19}$$

where c_t and c_p are the annual variable cost for the turbine and pump, respectively. The annual variable turbine cost represents the annual O&M cost and is determined from an expression developed by Mongird et al. [75] in which W_t is given in units of kW:

$$c_t = 15.9W_t + 0.00025E_{t_{annual}} \,. \tag{3.20}$$

The annual variable pump cost is given by

$$c_p = E_{p_{annual}}\, r_E + c_m \frac{E_{p_{annual}}}{1000} \tag{3.21}$$

where the first term represents the annual electricity cost required for operating the pump, and the second term represents the annual O&M cost of the pump. The parameters r_E and c_m are the electricity rate (assumed to be \$0.108/kWh [76]), and pump maintenance cost (assumed to be \$85/MWh-year [77]). Costs corresponding to structural system maintenance in both the BBGM and BBPH systems are not included as they are assumed to be negligible in comparison.

The other performance indicator utilized in this study is the variable storage cost (in \$/kWh). It is typically used for assessing the viability of grid-scale energy storage systems [75, 78], and can be expressed by the following relation [75]:

$$C_{se} = \frac{C}{E_{cycle}}. \tag{3.22}$$

The parameter E_{cycle} in Equation 3.22 represents the energy capacity stored over a single cycle and is given by

$$E_{cycle} = \frac{1}{2} W_t \sigma_{cycle} \,, \tag{3.23}$$

where W_t is given in units of kW.

The economic analysis described above for BBPH and BBGM scenarios is extended to include scenarios of the following two conventional rapidly deployable grid-scale energy generation and/or storage technologies: natural gas peaker plants (NGPP), and lithium-ion battery plants (LIBP). Table 3-6 shows the NGPP and LIBP scenario cost ranges used in the current analysis that correspond to the smallest BBGM energy capacity considered *(i.e.,* 50-m tall building with one column), and to the largest BBGM energy capacity considered (*i.e.,* 300-m tall building with 4 columns). The annual variable system costs for these technologies are calculated using equations 3.24 and 3.25, respectively.

$$c_{NGPP} = 13\, W_t + 0.0105\, E_{t_{annual}} + HR\, E_{t_{annual}}\, r_{NG}\,, \tag{3.24}$$

$$c_{LIBP} = 10\, W_t + 0.0003\, E_{t_{annual}} + \frac{E_{t_{annual}}}{\eta_{LIBP}} r_E\,. \tag{3.25}$$

The first and second terms in Equations 3.24 and 3.25 represent the fixed and variable annual O&M costs, respectively (obtained from [75]), and the third term represents the fuel/electricity cost. The parameter W_t in both equations is given in units of kW. The parameters HR, r_{NG}, and η_{LIBP} are the heat rate, natural gas rate, and LIBP roundtrip efficiency (assumed to be 0.01096 GJ/kWh, $2.52/GJ, and 86%, respectively [74, 78]). The values in Table 3-6 are used to calculate the LEC for the LIBP and NGPP scenarios using Equation 3.12. The denominator in Equation 3.12, which represents the annual energy output, is set to match the energy output of the BBGM configuration (*i.e.,* 1, 2, 3, or 4-columns) that is being compared against. The variable storage cost is not shown for the NGPP plant system as it is not a storage technology. A project lifetime of 50 years

is assumed with individual component lifetimes of 10 years for the LIBP system and 25 years for the NGPP system.

Table 3-6: Range of total capital system cost, C, annual variable system cost, c, and variable storage cost, C_{se}, used in NGPP and LIBP scenarios. All values include allowances for the cost of electromechanical equipment (required to operate the system) and installation.

System type	Parameter	Cost*
NGPP	C	\$54,871 - \$424,476 [1]
	c_{NGPP}	\$2,091/yr - \$47,098/yr
	C_{se}	\$469/kWh [1]
LIBP	C	\$27,377 – \$847,146 [2]
	c_{LIBP}	\$4,475/yr - \$128,295/yr

[1] Obtained from [75].

[2] Calculated using the following expression [75]: $C = 0.5 C_{se} W_t \sigma_{cycle}$, where W_t (in kW), and σ_{cycle} are set to match the power capacity and cycle time of the BBGM configuration (*i.e.,* 1, 2, 3, or 4-columns) that is being compared against, respectively.

3.2.9 Sensitivity analysis

The LEC of any given energy system can vary significantly based on the value of the input parameters assumed in the economic analysis (see Section 3.2.8) as these parameters are prone to vary in time due to impacts such as material/energy price volatility and/or inflation. A sensitivity analysis is conducted in the current study of a 150-meter tall BBGM system with 1 and 4 columns by varying the following key parameters: the total capital system cost, the electricity rate, the piston height, and the piston diameter. These parameters are used in the current analysis as their variation (assumed to be ± 60% in increments of 20%) is found to have the greatest impact on LEC. The selected range of variation is based on that which is used in a similar study by Merenjak and Krstic on the sensitivity analysis of facility's life cycle costs [37]. A preliminary analysis was also conducted of a 150-m tall BBPH system by varying the total capital system cost and electricity rate, and it was found that the sensitivity of the LEC was nearly identical to that

shown for the BBGM system, therefore the sensitivity results for the BBPH system are not shown in the current study.

3.3 Results and Discussion

Several insights are drawn from the current analysis which can be used to guide the design and direct future research into building-based energy storage systems. These insights are described in the following subsections.

Insight 1: *The LEC of BBGM and BBPH systems decreases as the building height increases. The BBGM system is capable of offering greater power capacity at a lower LEC than the BBPH system at all building heights analyzed.*

The LEC values corresponding to all BBPH and single-column BBGM scenarios described in Section 3.2.4 are shown in Figure 3-3. The BBGM system provides lower cost electricity than the BBPH system at all building heights analyzed.

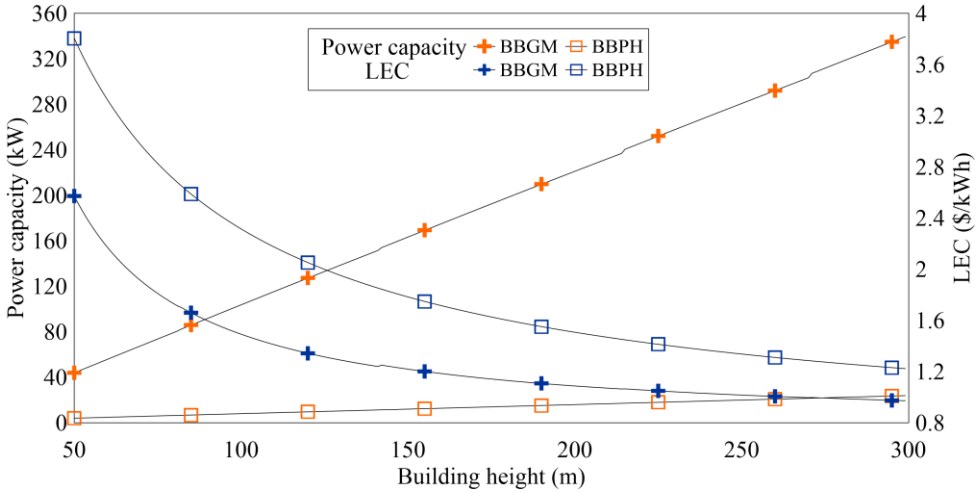

Figure 3-3: Variation of power capacity and LEC for BBGM (single-column) and BBPH systems as a function of building height.

The LEC of the BBPH and BBGM systems decreases from $3.8/kWh and $2.57/kWh at the lowest building height of 50 m to $1.22/kWh and $0.97/kWh at the tallest building height of 300 m, respectively. These reductions in the same order for the individual systems correspond to LEC differences of $2.58/kWh and $1.6/kWh over the entire building height range. This large shift in LEC in both systems is primarily due to the high system cost and low power production that is available in smaller buildings. Relative to each other, there is a LEC difference of $1.23/kWh at the lowest building height, and $0.25/kWh at the tallest building height. Therefore, even a slight increase in power capacity causes the LEC of the BBPH system to reduce more rapidly than that of the BBGM system. Figure 3-3 also shows that the power capacity of the BBGM and BBPH systems increases linearly from 43.9 to 339.5 kW, and 4 to 23.8 kW, respectively, across the full building height range. The greater increase in power capacity for the BBGM system is directly related to the volume of water which increases in the gravity module column as a function of building height. This effect is not present in the BBPH system as the reservoir volume remains fixed regardless of the building height. Overall, the increased power capacity and energy density of the BBGM system outweighs the higher costs incurred by the piston and column, which makes this system less costly than the BBPH system.

Insight 2: *The LEC of the BBGM system decreases as the number of columns added to the system increases, however the % decrease associated with each incremental column addition is marginally less.*

The LEC values corresponding to all multi-column BBGM scenarios described in Section 3.2.5 are shown in Figure 3-4. For all multi-column configurations (*i.e.,* 2, 3, and

4-column systems), the LEC decreases as the building height increases. The LECs of the 2, 3, and 4-column BBGM configurations decrease from \$2.37/kWh, \$2.30/kWh, and \$2.27/kWh at the lowest building height of 50 m to \$0.86/kWh, \$0.82/kWh, and \$0.80/kWh at the tallest building height of 300 m, respectively. However, the overall decrease in LEC for the multi-column BBGM configuration is not as great as that of the single-column configuration across all building heights. Increasing the building height from 50 to 300 m for the 2, 3, and 4-column BBGM configurations causes the LEC to decrease by roughly \$1.51/kWh, \$1.48/kWh, and \$1.47/kWh, respectively. These values are moderately less than the overall decrease corresponding to the one-column configuration which is approximately \$1.6/kWh.

Figure 3-4 also shows that there is a noticeable diminishing returns effect from adding additional columns to the BBGM system (*i.e.,* adding more columns results in a more profitable system up to a point where the economic gains start to become negligible). The average LECs corresponding to the 1, 2, 3, and 4-column BBGM configurations across the full building height range are roughly \$1.28/kWh, \$1.16/kWh, \$1.12/kWh, and \$1.09/kWh, respectively. Relative to the 1-column configuration, these average LEC values in the order given are lower by approximately 9.4%, 12.5%, and 14.8%. The reason the average LEC is lower in systems that contain more columns is mainly due to the system's geometry. Multi-column BBGM systems contain a single centralized penstock, therefore as the system increases in size (*i.e*., more columns are added), the system capital costs are more evenly divided across the total system's energy generation and storage capacity.

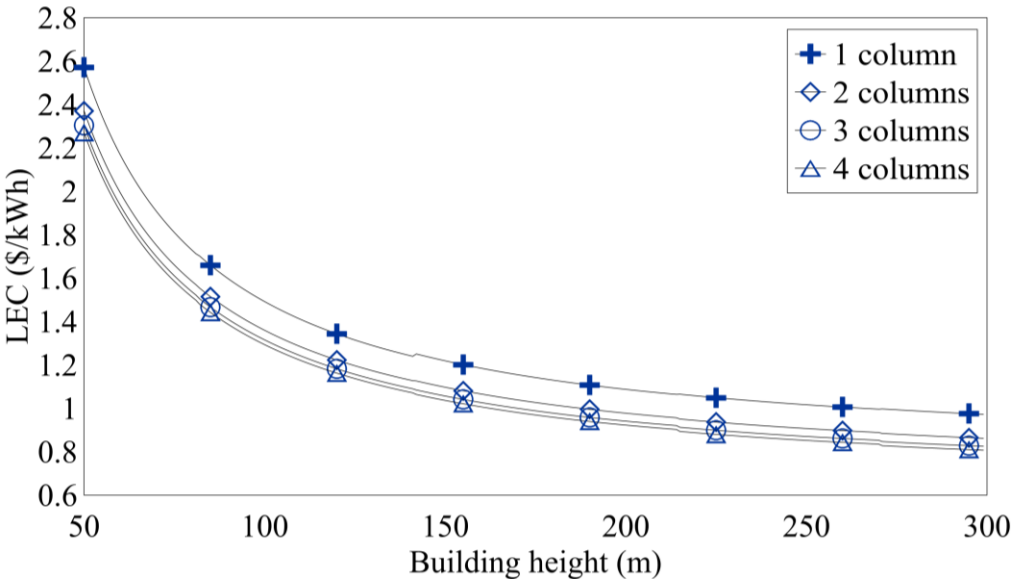

Figure 3-4: Variation of LEC for multi-column BBGM configurations as a function of building height.

Insight 3: *High on-demand power and energy capacities are available in tall multi-column BBGM systems. Building operators can potentially leverage these systems to gain profit by participating in the electrical grid capacity and energy storage markets (if applicable in the given jurisdiction).*

Figure 3-5 shows the power capacities and energy cycle capacities, E_{cycle}, of multi-column BBGM configurations as a function of building height. For all configurations, increasing the building height causes the power capacity to increase linearly. For example, the power capacity at the lowest building height of 50 m for the 1, 2, 3, and 4-column configurations is 43.9 kW, whereas this same value at the tallest building height of 300 m is 339.5 kW. Furthermore, the power capacity between each configuration at any given building height remains constant. This is not the case, however, for the energy cycle capacities of the different configurations. Although increasing the building height causes

the energy cycle capacity to increase linearly, the difference in energy cycle capacity between each configuration at any given building height increases as the number of columns increases. For example, the energy cycle capacities at the lowest building height of 50 m for the 1, 2, 3, and 4-column configurations are 43.9 kWh, 87.8 kWh, 131.7 kWh, and 175.6, kWh, whereas these same values at the tallest building height of 300 m are 339.5 kWh, 679.1 kWh, 1,017 kWh, and 1,358 kWh, respectively. The reason for this increase in energy cycle capacity between configurations is due to the longer charge/discharge time assumed for multi-column BBGM scenarios (see Section 3.2.5).

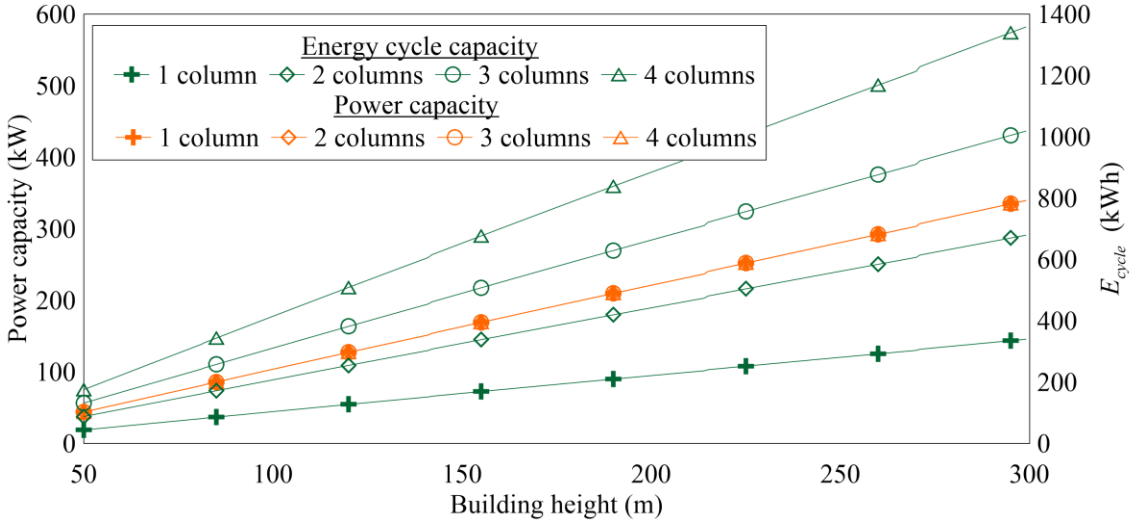

Figure 3-5: Power capacity and energy cycle capacity, E_{cycle}, of multi-column BBGM configurations as a function of building height.

Building operators can potentially leverage these systems to gain profit by participating in one or more jurisdiction-dependent electricity markets such as the capacity market, or the energy storage market. The capacity market offers bidders (in the current case - building operators) an opportunity to sell electricity to the grid within a deregulated energy system. Bids to sell electricity are typically fixed at the marginal cost of generation, and the amount paid out to the bidder is equivalent to the market-clearing price. If the

market clearing price is above the bidder's marginal cost of generation, then the difference between these two values is earned as profit [80, 81]. A strategy for operating BBGM systems profitably within this context involves selling electricity (*i.e.*, discharging the BBGM system) during peak load periods and buying electricity (*i.e.,* charging the BBGM system) during off-peak periods. Even greater profits can potentially be earned by participating in the energy storage market that is frequently used by utilities to access energy storage capacity and thereby gain flexibility and cost savings [82].

Insight 4: *The LEC of BBGM systems is highly sensitive to changes in total capital system cost and electricity rate.*

Figure 3-6 shows the percent change in LEC of a 150-meter tall BBGM system with a) 1 column, and b) 4 columns as a result of varying the following key parameters by ± 60%: the total capital system cost, the electricity rate, the piston height, and the piston diameter. Varying these parameter values (in the order given) across the entire range causes the percent change in LEC to vary between -45% and 45%, -7.4% and 7.4%, 47% and -10.8%, and 47% and -9% for the single-column configuration. Similarly, for the 4-column configuration, the percent change in LEC varies between -44% and 44%, -8.7% and 8.7%, 42% and -8.6%, and 21% and -3.6%. Overall, these results show that increasing the total capital system cost and electricity rate causes the LEC to increase, whereas, increasing the piston height and the piston diameter causes the LEC to decrease. Figure 3-6 also shows that the LEC of the single-column configuration is more sensitive to changes in piston diameter than the 4-column configuration. This effect is mainly due to the ratio between the total cost and energy capacity of the system. On the other hand, the LEC of the 4-

column configuration is more sensitive to changes in total electricity rate than the single-column configuration. This is mainly due to the pump in the 4-column configuration using significantly more energy for charging the system.

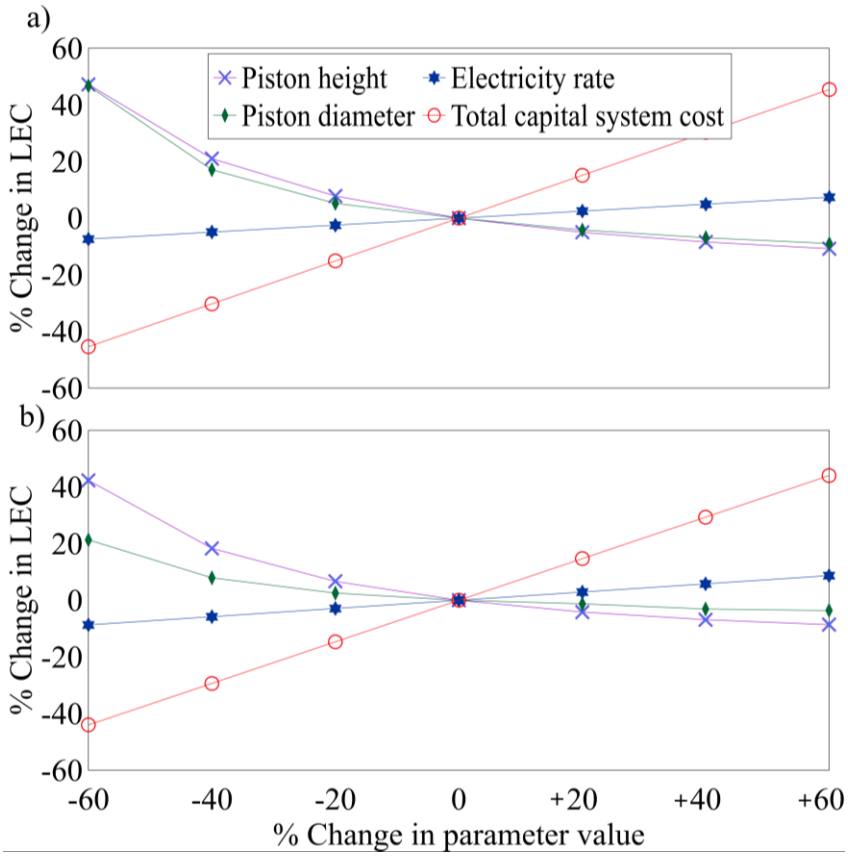

Figure 3-6: Percent change in LEC of a 150-meter tall BBGM system with a) 1 column, and b) 4 columns as a result of varying the total capital system cost, the electricity rate, the piston height, and the piston diameter by ± 60%.

Insight 5: *The LEC of 3 and 4-column BBGM systems is lower than that of BBPH and LIBP systems in buildings that are taller than 163 m and 156 m. As a performance metric for gauging the economic viability of energy storage systems, the LEC is better than the variable storage cost as it considers system lifetime costs and the time value of money.*

Figure 3-7 shows the variable storage cost, C_{se}, ($/kWh) and corresponding energy cycle capacity (kWh) for BBGM, LIBP and BBPH scenarios as a function of building height. BBGM scenarios with a) 1 column, b) 2 column, c) 3 column, and d) 4 column configurations are compared with the LIBP scenarios on an equivalent energy cycle capacity basis. NGPP scenarios are not shown in Figure 3-7 as these plants do not store energy. For all BBPH and BBGM scenarios, increasing the building height causes the variable storage cost to decrease. The variable storage cost corresponding to the LIBP system, on the other hand, remains constant in all scenarios. The LIBP system has the lowest variable storage cost of all systems considered in this study, and has a value of $624/kWh. This value is in line with the average utility-scale battery variable storage cost of $831/kWh published by the U.S. Energy Information Administration (EIA) [83]. The variable storage cost of the BBPH system, which is identical at any given building height from a) to d), decreases from $35,448/kWh at the lowest building height of 50 m to $11,394/kWh at the tallest building height of 300 m. The variable storage cost of the 1, 2, 3, and 4-column BBGM configurations decrease from $21,229/kWh, $19,482/kWh, $18,900/kWh, and $18,609/kWh to $6,264/kWh, $5,365/kWh, $5,066/kWh, and $4,916/kWh, respectively, across this same building height range.

The costs mentioned above for BBPH and BBGM systems greatly exceed the variable storage cost upper range value of $1,946/kWh provided by the EIA which covers

a large array of conventional storage technologies. This is mainly due to the high capital cost associated with BBPH and BBGM systems. The variable storage costs corresponding to the BBGM systems in the current study are also well above the $1,103/kWh and $3,099/kWh values identified by Oldenmenger [6] for these same systems. This discrepancy can be explained by the difference in assumptions utilized in both studies. In Oldenmenger's study, a 48 m tall piston is utilized that is made of inexpensive ($152/tonne) and highly dense (5,500 kg/m^3) metal. In the current study, a more conservative approach is taken in which a 13.5 m tall piston is assumed that is made of steel (7,871 kg/ m^3) that has a much higher material cost ($931/tonne).

From an energy cycle capacity standpoint, all scenarios shown in Figure 3-7 are directly comparable except for those of the BBPH system. BBPH scenario variations are identical in Figures 3-7a to 3-7d since the energy storage capacity of the upper reservoir on the building's roof is fixed. Since BBPH systems have the lowest energy cycle capacity (at any given building height) and the lowest variable storage cost, these systems provide little value relative to the other technologies investigated in this study. BBGM systems, on the other hand, have much greater energy cycle capacities (especially in multi-column configurations), and are therefore much more beneficial despite their high associated variable storage cost.

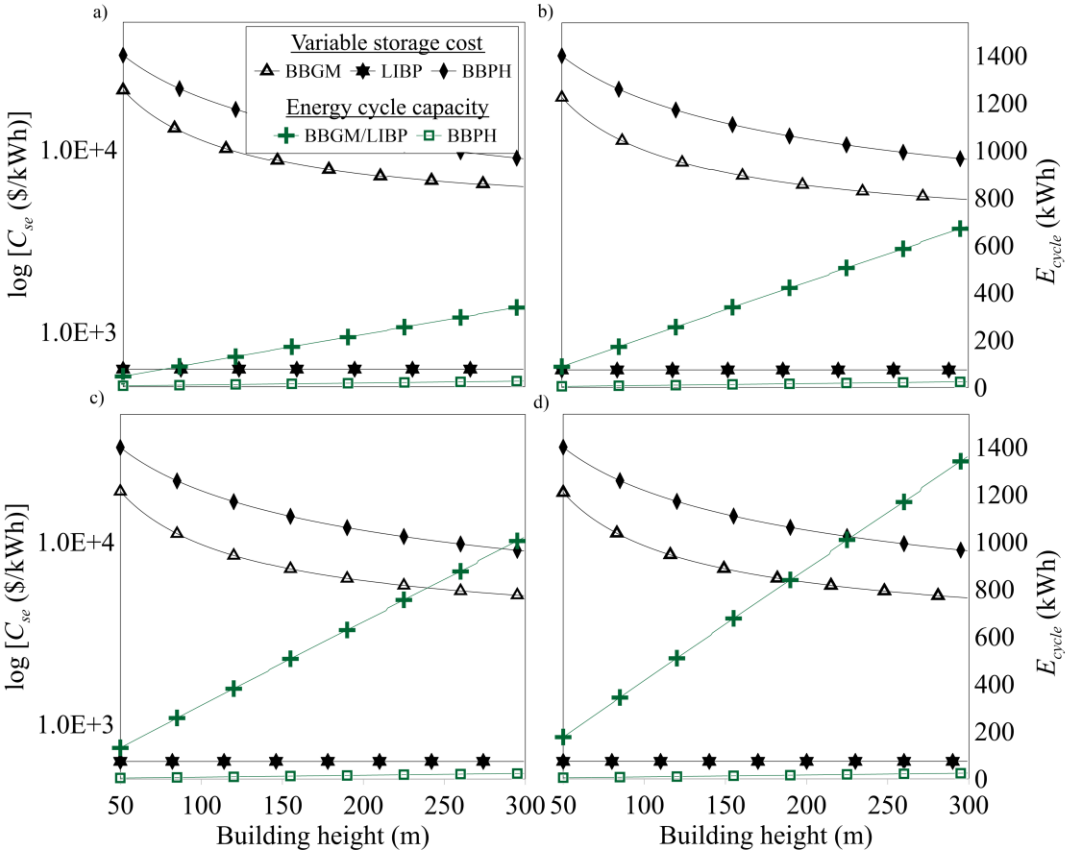

Figure 3-7: Variable storage cost, C_{se}, ($/kWh) and energy cycle capacity, E_{cycle}, (kWh) of BBGM, LIBP and BBPH scenarios as a function of building height. BBGM scenarios with a) 1 column, b) 2 column, c) 3 column, and d) 4 column configurations are compared with the LIBP scenarios on an equivalent energy capacity basis. BBPH scenario variations are identical in a) to d).

Although the variable storage cost is the most commonly used metric for comparing alternative storage technologies, it is highly limited in that it does not include costs and benefits that are incurred during the lifetime of the energy system (*i.e.,* it is only a function of capital cost and energy cycle capacity), nor does it consider the time value of money. The LEC is therefore potentially better suited as a metric for comparing the economic viability of grid-scale energy storage technologies as these factors are considered.

Figure 3-8 shows the levelized electricity cost, LEC, ($/kWh) and corresponding energy cycle capacity (kWh) of BBGM, BBPH, LIBP, and NGPP scenarios as a function

of building height. BBGM scenarios with a) 1 column, b) 2 column, c) 3 column, and d) 4 column configurations are compared with the LIBP and NGPP scenarios on an equivalent energy cycle capacity basis. For all configurations, increasing the building height (or energy capacity for LIBP and NGPP systems) causes the LEC to decrease. Although the decrease in LEC is significant as a function of building height for BBGM and BBPH systems, no change is observed for LIBP and NGPP systems. The LEC of the BBPH system, which is identical at any given building height in Figures 3-8a to 3-8d, decreases from $3.8/kWh at the lowest building height of 50 m to $1.22/kWh at the tallest building height of 300 m. This system is the least economical of all systems considered in this study from an LEC standpoint. The NGPP system, on the other hand, is generally the most economical of all systems considered, however, it should be noted that this technology is not a storage technology like the other systems under comparison. The average LEC of the NGPP system decreases from $1.84/kWh to $0.49/kWh, in Figures 3-8a and 3-8d, respectively. This decrease is due to the low fixed and variable cost of NGPP systems (whose impact is especially apparent at higher energy capacities).

The LEC of the 1, 2, 3, and 4-column BBGM configurations decrease from $2.57/kWh, $2.37/kWh, $2.3/kWh, and $2.27/kWh to $0.97/kWh, $0.86/kWh, $0.82/kWh, and $0.80/kWh, respectively, from building heights of 50 m to 300 m. The LEC of the LIBP system remains constant with a value of approximately $1.02/kWh in Figures 3-8a and 3-8d, respectively. Generally, when energy storage is a requirement, the LIBP system is the most economical system when compared against BBGM systems of lower building heights. However, the BBGM system becomes more economical than the LIBP system at these low building heights as the number of gravity module columns

increases. For example, the LEC of the 1, 2, 3, and 4-column BBGM system is lower than that of the LIBP system at building heights of 241 m, 178 m, 163 m, and 156 m, respectively. To put these values into context, there are roughly 29 buildings that are taller than 156 m in the Canadian cities of Vancouver and Toronto alone.

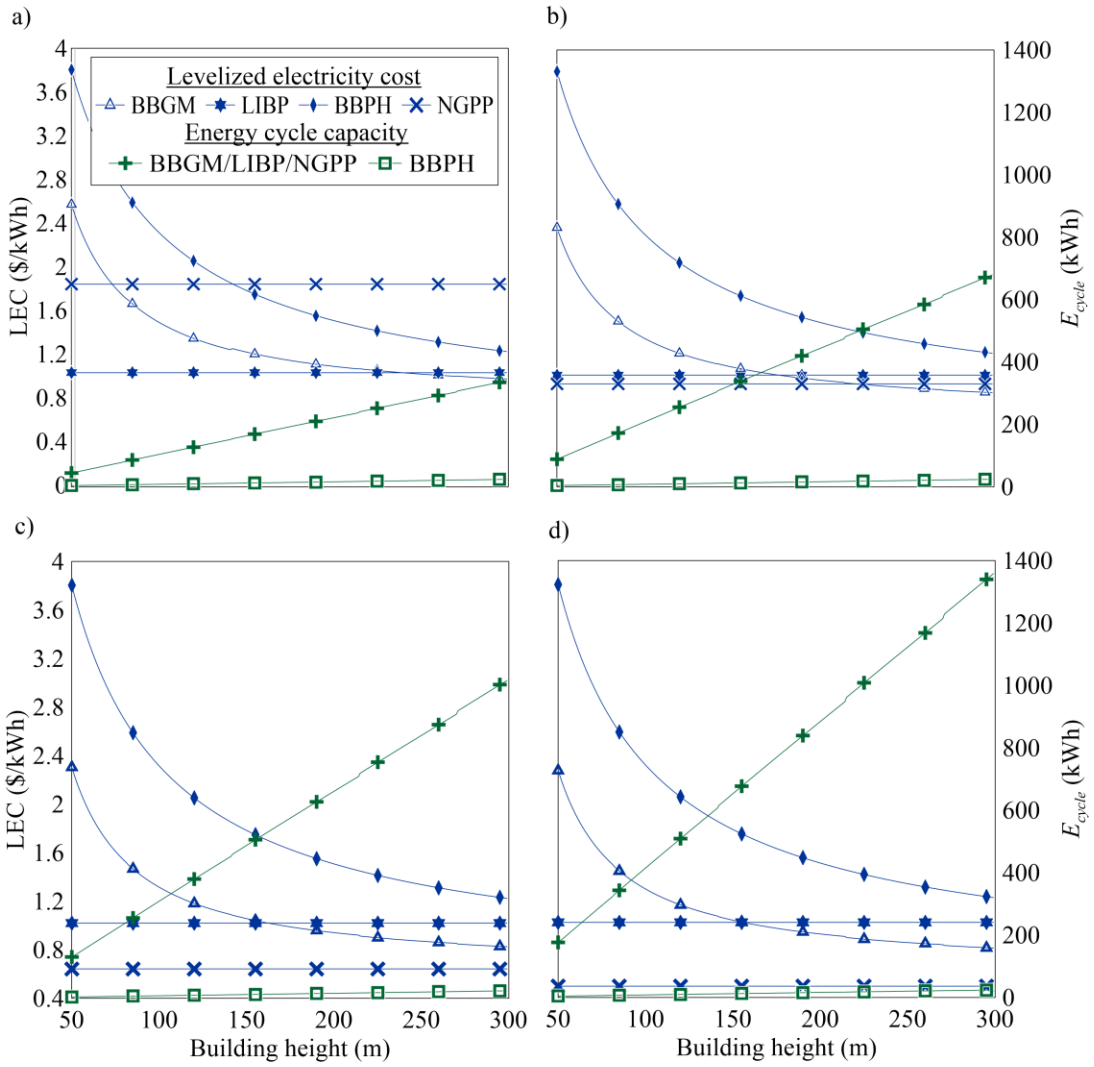

Figure 3-8: Levelized electricity cost, LEC, ($/kWh) and energy cycle capacity, E_{cycle}, (kWh) of BBGM, BBPH, LIBP and NGPP scenarios as a function of building height. BBGM scenarios with a) 1 column, b) 2 column, c) 3 column, and d) 4 column configurations are compared with the LIBP and NGPP scenarios on an equivalent energy cycle capacity basis. BBPH scenario variations are identical in a) to d).

Based on the above LEC analysis, BBGM systems can be seen as a preferable alternative to LIBP systems depending on the system's configuration (*e.g.,* number of columns) and associated building height. This finding differs greatly from the trend shown in Figure 3-7 which shows the variable storage cost of LIBP systems being lower than that of BBGM systems in all scenarios considered. This result brings to light the importance of utilizing an economic metric that accounts for system lifetime costs and the time value of money when assessing the viability of rapidly deployable grid-scale energy generation and/or storage solutions.

Although the current study provides a general understanding of the advantages and disadvantages of implementing the proposed building-based hydroelectric storage systems from a techno-economic standpoint, the following questions are left unanswered (which could potentially formulate the basis of future research):

- What are the structural requirements associated with these systems, and how would building codes be affected in different jurisdictions?,
- What impacts would the large-scale implementation of these distributed storage systems have on the electrical grid, and what value can be gained from building operators and/or the electrical utility?,
- How much interior building space would be required to house system equipment, and what impact would this have on the available floor space?, and
- What policy mechanisms are needed to incentivize the widespread implementation of these systems?

3.4 Conclusions

This study assessed the techno-economic performance of BBPH and single and multiple-column BBGM systems as a function of building height (from 50 – 300 m), and compared these systems with two conventional rapidly deployable grid-scale energy generation and/or storage technologies: natural gas peaker plants (NGPP), and lithium-ion battery plants (LIBP). System performance was quantified via the power and energy cycle capacity, the variable storage cost, and the levelized electricity cost. The following key insights were obtained from the analysis:

- The LEC of BBGM and BBPH systems decreases as the building height increases (*e.g.,* the LEC of a 1-column BBGM decreases from $2.57/kWh at a building height of 50 m to $0.97/kWh at a building height of 300 m), and BBGM systems (single and multi-column) are capable of offering greater power capacity at a lower LEC than BBPH systems.
- The LEC of BBGM systems decreases as the number of columns added to the system increases. For example, the LEC of a 300 m tall BBGM system is $0.97/kWh in a 1-column configuration versus $0.80/kWh in a 4-column configuration.
- Tall multi-column BBGM systems are able to provide significant on-demand power and energy (*e.g.,* 339.5 kW and 1,358 kWh, respectively, for a 300 m tall 4-column configuration), which may potentially be an asset to building operators wishing to earn profit by participating in the electrical capacity and/or storage markets (if available).

- The LEC of BBGM systems is highly sensitive to changes in total capital system cost and electricity rate. For example, increasing these parameters in the given order by 60% causes the LEC to increase by 44% and 8.7%.
- The LEC of 3 and 4-column BBGM systems is lower than that of LIBP systems in buildings that are taller than 163 m and 156 m, respectively.
- LEC is a more complete metric than the variable storage cost for gauging the economic viability over the lifetime of energy storage systems as it considers system lifetime costs and the time value of money.

The findings obtained from this study demonstrate the techno-economic tradeoffs that exist between BBPH, BBGM, LIBP, and NGPP systems, and show that building-based hydroelectric storage systems are comparable (and in some cases preferable) to conventional rapidly deployable grid-scale energy generation and/or storage systems. The potential benefits of implementing these systems on a citywide scale have yet to be determined.

Chapter 4: Summary of contributions

This thesis investigates the technical and economic feasibility of implementing two alternative hydroelectric generation systems into high-rise buildings. A summary of contributions from each chapter of this thesis is outlined below.

4.1 Chapter 2: Performance evaluation of a residential building-based hydroelectric system driven by wastewater

This chapter investigated the techno-economic feasibility of implementing a hydroelectric generation system in the wastewater system of a high-rise building. A numerical model developed in the Matlab/Simscape™ environment was used to conduct simulations using measured water consumption data from a case study building in Ottawa, Canada. The data was then extrapolated to 2,400 additional scenarios that correspond to buildings that contain between 15 and 75 floors, with 10 to 50 units per floor. The main contributions/findings of this chapter are as follows:

- Implementing a building-based wastewater hydroelectric system can offset the total annual pumping energy requirement by up to 36% regardless of the building's height.
- Increasing the electricity rate has the single largest positive impact on the cost-effectiveness of the wastewater hydroelectric system for a building of a given size.
- Both the annual energy generation and system cost-effectiveness increase as the building size increases. Under Ontario's average electricity rate, the financial breakeven point occurs in buildings that have a minimum of 35 floors with at least

47 units per floor. Conversely, under a higher average electricity rate such as that encountered in California, this breakeven point occurs in smaller buildings.

- Incorporating the proposed wastewater hydroelectric system in new buildings worldwide can provide significant local energy generation potential as major cities continue to densify and expand upwards.

4.2 Chapter 3: Evaluation of building-based hydroelectric systems as a rapidly deployable grid-scale energy storage solution

This chapter assessed the techno-economic performance of BBPH and single and multiple-column BBGM systems as a function of building height (from 50 – 300 m), and compared these systems with two conventional rapidly deployable grid-scale energy generation and/or storage technologies: natural gas peaker plants (NGPP), and lithium-ion battery plants (LIBP). System performance was quantified via the power and energy cycle capacity, the variable storage cost, and the levelized electricity cost. The following key insights were obtained from the analysis:

- The LEC of BBGM and BBPH systems decreases as the building height increases (*e.g.,* the LEC of a 1-column BBGM decreases from $2.57/kWh at a building height of 50 m to $0.97/kWh at a building height of 300 m), and BBGM systems (single and multi-column) are capable of offering greater power capacity at a lower LEC than BBPH systems.
- The LEC of BBGM systems decreases as the number of columns added to the system increases. For example, the LEC of a 300 m tall BBGM system is

$0.97/kWh in a 1-column configuration versus $0.80/kWh in a 4-column configuration.

- Tall multi-column BBGM systems are able to provide significant on-demand power and energy (*e.g.,* 339.5 kW and 1,358 kWh, respectively, for a 300 m tall 4-column configuration), which may potentially be an asset to building operators wishing to earn profit by participating in the electrical capacity market.
- The LEC of BBGM systems is highly sensitive to changes in total capital system cost and electricity rate. For example, increasing these parameters in the given order by 60% causes the LEC to increase by 44% and 8.7%.
- The LEC of 3 and 4-column BBGM systems is lower than that of LIBP systems in buildings that are taller than 163 m and 156 m, respectively.
- LEC is a better metric than the variable storage cost for gauging the economic viability of energy storage systems as it considers system lifetime costs and the time value of money.

Chapter 5: Recommendations and future work

Throughout this research project, additional questions arose pertaining to unresolved issues and topics that warrant further study. Unresolved issues are discussed in detail at the end of Chapters 2 and 3. A few key recommendations for future work are presented as follows:

- In the current thesis, the value of electricity generated or stored is associated with specific pricing programs. However, there are a multitude of different pricing strategies and energy markets used to value electricity that are dependent on factors such as jurisdiction, demand, and generation capabilities. Further research into the value of distributed electricity generation and storage at an urban scale in different energy markets may potentially result in increased economic value of the proposed systems.
- This thesis does not consider the internal building space that is occupied by the proposed systems when conducting the economic analysis. Further research into the volumetric requirements of these systems and the associated value of area that these systems displace could potentially have a considerable impact on the results.
- The wastewater hydroelectric system is assumed to include a single small tank and turbine configuration, and the BBGM and BBPH systems have a fixed piston/reservoir size. These sizing constraints are implemented to lower the number of possible scenarios in the thesis, however there is a possibility that different configurations could offer more value. Alternate component sizes should therefore be considered.

- The current thesis assumes that the installation of a reservoir or BBGM column is possible using existing building methods. Additionally, building codes and regulations have not been considered as these are likely to change from one jurisdiction to another. Of particular importance is the issue of placing a wastewater collection tank indoors and the differences between combined wastewater tanks, and that of separate black and grey water tank. Similarly, the impact of discharging wastewater collection tanks from multiple buildings on the local surrounding sewer system is currently unknown. Further work regarding the code regulations surrounding the proposed wastewater and energy storage systems are recommended.

Chapter 6: Conclusion

This thesis evaluated the potential for high-rise building-based hydroelectric generation and storage over a variety of different building sizes to determine their technological and economic viability.

In Chapter 2, the techno-economic performance of a wastewater driven hydroelectric system was investigated using a case study building in Ottawa, Canada. Historical water usage data was used to create a schedule that dictated the temporal availability of water for energy generation. Using this data, 2,400 additional model scenarios were considered that correspond to buildings that contain between 15 and 75 floors, with 10 to 50 units per floor. As part of the technical analysis, the annual pumping energy requirement and the annual turbine energy generation were calculated. It was determined that installing a wastewater hydroelectric turbine would increase the efficiency of a building's water delivery system by up to 36%. Results from the economic analysis showed that buildings with a minimum of 35 floors with at least 47 units per floor had a positive financial return, and that the electricity rate under a time-of-use rate structure had the highest impact on this value.

In Chapter 3, BBPH and BBGM systems were analyzed as a function of building height (50-300 m) and compared on the basis of system power, energy capacity, and LEC. These systems were compared to equivalent conventional rapidly deployable grid-scale energy storage and generation systems: lithium-ion battery plants (LIBP) and natural gas peaker plants (NGPP). It was determined that the BBGM system provided higher energy capacities and lower levelized energy costs than the BBPH system. Also, the BBGM's energy capacity increased (and LEC decreased) as more modules were added to a building.

Relative to LIBPs, multi-column BBGM systems were found to be a more cost-effective option in buildings that are taller than 156 m.

Overall, this thesis presented the potential techno-economic benefits of building-based wastewater hydroelectric systems, and building-based energy storage systems. The findings show that these systems have the potential to be implemented on a large scale possibly leading to significant energy and cost savings. However, research is still needed from both a technical and policy standpoint to gauge the true impact of these systems in our current and future energy landscape.

References

[1] "1 USD to CAD | Convert US Dollars to Canadian Dollars | Xe." [Online]. Available: https://www.xe.com/currencyconverter/convert/?Amount=1&From=USD&To=CAD. [Accessed: 29-Mar-2021].

[2] S. G. Santillan, "Creating Renewable Energy in a Residential High-Rise by Utilizing Greywater in a Hydropower Turbine," M.S. Thesis, School of Arch. Univ. of Arizona., Tucson, 2016.

[3] T. M. Müller, P. Leise, I. S. Lorenz, L. C. Altherr, and P. F. Pelz, "Optimization and validation of pumping system design and operation for water supply in high-rise buildings," *Optim. Eng.*, vol. 22, no. 2, pp. 643–686, 2020.

[4] J. D. Hunt, E. Byers, Y. Wada, S. Parkinson, D. E. H. J. Gernaat, S. Langan, D. P. van Vuuren, and K. Riahi, "Global resource potential of seasonal pumped hydropower storage for energy and water storage," *Nat. Commun.*, vol. 11, no. 1, pp. 1–8, 2020.

[5] A. Z. AL Shaqsi, K. Sopian, and A. Al-Hinai, "Review of energy storage services, applications, limitations, and benefits," *Energy Reports*, vol. 6, pp. 288–306, 2020.

[6] A. W. Oldenmenger, "Highrise Energy Storage Core: Feasibility study for a hydro-electrical pumped energy storage system in a tall building," M.S. Thesis, Dept. of Civ. Eng. and GeoSc., Delft University of Technology., Delft, Netherlands, 2013.

[7] S. Nag, K. Y. Lee, and D. Suchitra, "A comparison of the dynamic performance of conventional and ternary pumped storage hydro," *Energies*, vol. 12, no. 18, 2019.

[8] M. Simão and H. M. Ramos, "Hybrid pumped hydro storage energy solutions

towards wind and PV integration: Improvement on flexibility, reliability and energy costs," *Water (Switzerland)*, vol. 12, no. 9, 2020.

[9] C.-J. Yang and R. Jackson, "Opportunities and barriers to pumped-hydro energy storage in the United States," *Renew. Sustain. Energy Rev.*, vol. 15, pp. 839–844, Jan. 2011.

[10] "A New Approach to Pumped Storage Hydropower | Department of Energy." [Online]. Available: https://www.energy.gov/eere/water/articles/new-approach-pumped-storage-hydropower. [Accessed: 30-Oct-2021].

[11] A. Blakers, M. Stocks, B. Lu, and C. Cheng, "A review of pumped hydro energy storage Andrew," *Prog. Energy*, vol. 3, no. 2, 2021.

[12] A. J. Pimm, T. T. Cockerill, and P. G. Taylor, "The potential for peak shaving on low voltage distribution networks using electricity storage," *J. Energy Storage*, vol. 16, pp. 231–242, 2018.

[13] P. Sarkar, B. Sharma, and U. Malik, "Energy generation from grey water in high raised buildings: The case of India," *Renew. Energy*, vol. 69, pp. 284–289, 2014.

[14] J. Titus and B. Ayalur, "Design and fabrication of in-line turbine for pico hydro energy recovery in treated sewage water distribution line," *Energy Procedia*, vol. 156, no. September 2018, pp. 133–138, 2019.

[15] J. Zhang and Q. Zhang, "High-rise building mini-hydro pumped-storage scheme with Shanghai Jinmao Tower as a case study," *IEEE Power Energy Soc. Gen. Meet.*, vol. 2014-Octob, no. October, 2014.

[16] G. de Oliveira e Silva and P. Hendrick, "Pumped hydro energy storage in buildings," *Appl. Energy*, vol. 179, pp. 1242–1250, 2016.

[17] A. C. Ruoso, N. R. Caetano, and L. A. O. Rocha, “Storage gravitational energy for small scale industrial and residential applications,” *Inventions*, vol. 4, no. 4, pp. 1–13, 2019.

[18] K. Loudiyi and A. Berrada, “Experimental Validation of Gravity Energy Storage Hydraulic Modeling,” *Energy Procedia*, vol. 134, pp. 845–854, 2017.

[19] “Natural gas generators make up the largest share of overall U.S. generation capacity - Today in Energy - U.S. Energy Information Administration (EIA).” [Online]. Available: https://www.eia.gov/todayinenergy/detail.php?id=34172. [Accessed: 30-Oct-2021].

[20] C. Dortans, M. W. Jack, B. Anderson, and J. Stephenson, “Lightening the load: quantifying the potential for energy-efficient lighting to reduce peaks in electricity demand,” *Energy Effic.*, vol. 13, no. 6, pp. 1105–1118, 2020.

[21] “Electricity and Energy Storage - World Nuclear Association.” [Online]. Available: https://world-nuclear.org/information-library/current-and-future-generation/electricity-and-energy-storage.aspx. [Accessed: 17-May-2021].

[22] Government of Ontario, “Design Guidelines for Drinking-Water Systems: Instrumentation & control and distribution systems | Ontario.ca,” 2021. [Online]. Available: https://www.ontario.ca/document/design-guidelines-drinking-water-systems/instrumentation-control-and-distribution-systems. [Accessed: 12-Jul-2021].

[23] Bell & Gossett, “Parallel and Series Pump Application,” p. 18, 2012.

[24] A. Steele, “High-Rise Domestic Water Systems,” *Continuing education: Plumbing Systems & Design*, pp. 26–32, 2003.

[25] B. Hendron and J. Burch, “Tool for Generating Realistic Residential Hot Water Event Schedules,” in *National Renewable Energy Laboratory*, New York, 2010, no. August.

[26] P. W. Mayer, W. B. DeOreo, E. Towler, and D. M. Lewis, “Residential Indoor Water Conservation Study: Evaluation of High Efficiency Indoor Plumbing Fixture Retrofits in Single-Family Homes in the East Bay Municipal Utility District Service Area,” Boulder, 2003.

[27] Mathworks, “Solve moderately stiff ODEs and DAEs — trapezoidal rule - MATLAB ode23t,” 2021. [Online]. Available: https://www.mathworks.com/help/matlab/ref/ode23t.html. [Accessed: 01-Apr-2021].

[28] L. Zeghadnia, J. L. Robert, and B. Achour, “Explicit solutions for turbulent flow friction factor: A review, assessment and approaches classification,” *Ain Shams Eng. J.*, vol. 10, no. 1, pp. 243–252, 2019.

[29] M. F. Basar, R. Sapiee, S. Rahman, Z. Hamdan, S. Borhan, and K. Sopian, “Cost analysis of pico hydro turbine for power production,” *Adv. Environ. Biol.*, vol. 8, no. 14, pp. 147–151, 2014.

[30] P. W. O’Connor, Q. F. Zhang, S. T. DeNeale, D. R. Chalise, E. Centurion, and A. Maloof, “Hydropower baseline cost modeling, Version 2,” 2015.

[31] A. Immendoerfer, I. Tietze, H. Hottenroth, and T. Viere, “Life-cycle impacts of pumped hydropower storage and battery storage,” *Int. J. Energy Environ. Eng.*, vol. 8, no. 3, pp. 231–245, 2017.

[32] RS Means Company, *RS Means Plumbing Costs*, 39th ed. Rockland: Construction

Publishers and Consultants, 2016.

[33] Homeguide, “2020 Septic Tank Pumping Cost | Average Cleaning & Emptying Cost,” 2020. [Online]. Available: https://homeguide.com/costs/septic-tank-pumping-cost. [Accessed: 21-Apr-2020].

[34] United States Environmental Protection Agency, “How to Care for Your Septic System | Septic Systems (Onsite/Decentralized Systems) | US EPA,” 2021. [Online]. Available: https://www.epa.gov/septic/how-care-your-septic-system. [Accessed: 07-Jun-2021].

[35] Hydro Ottawa, “Residential Rates | Hydro Ottawa,” 2021. [Online]. Available: https://hydroottawa.com/en/accounts-services/accounts/rates-conditions/residential-rates. [Accessed: 29-Mar-2021].

[36] B. Steffen, “Estimating the cost of capital for renewable energy projects,” *Energy Economics*, vol. 88. Elsevier, 2020.

[37] S. Marenjak and H. Krstić, “Sensitivity analysis of facilities life cycle costs,” *Teh. Vjesn.*, vol. 17, no. 4, pp. 481–487, 2010.

[38] R. Martin, I. Lazakis, S. Barbouchi, and L. Johanning, “Sensitivity analysis of offshore wind farm operation and maintenance cost and availability,” *Renew. Energy*, vol. 85, pp. 1226–1236, 2016.

[39] J. Aldersey-Williams and T. Rubert, “Levelised cost of energy – A theoretical justification and critical assessment,” *Energy Policy*, vol. 124, no. October 2018, pp. 169–179, 2019.

[40] L. Ji, X. Liang, Y. Xie, G. Huang, and B. Wang, “Optimal design and sensitivity analysis of the stand-alone hybrid energy system with PV and biomass-CHP for

remote villages," *Energy*, vol. 225, p. 120323, 2021.

[41] Hydro Quebec, "Comparison of electricity prices in major North American cities," 2014.

[42] SkyscraperPage, "Canada - SkyscraperPage.com," 2021. [Online]. Available: https://skyscraperpage.com/database/country/1. [Accessed: 19-Nov-2019].

[43] RDHBuilding Engineering Ltd, "Energy Consumption and Conservation in Mid and High Rise Residential Buildings in British Columbia," vol. 1, p. 264, 2012.

[44] J. Aleksiejuk-Gawron, S. Milčiuviene, J. Kiršiene, E. Doheijo, D. Garzon, R. Urbonas, and D. Milčius, "Net-metering compared to battery-based electricity storage in a single-case pv application study considering the lithuanian context," *Energies*, vol. 13, no. 9, 2020.

[45] Ontario Energy Board, "What initiatives are available? | Ontario Energy Board," 2021. [Online]. Available: https://www.oeb.ca/industry/tools-resources-and-links/information-renewable-generators/what-initiatives-are-available. [Accessed: 01-Apr-2021].

[46] H. Shareef, M. S. Ahmed, A. Mohamed, and E. Al Hassan, "Review on Home Energy Management System Considering Demand Responses, Smart Technologies, and Intelligent Controllers," *IEEE Access*, vol. 6, pp. 24498–24509, 2018.

[47] Pacific Gas & Electric, "Residential Rates Plan Pricing," 2021. [Online]. Available: https://www.pge.com/pge_global/common/pdfs/rate-plans/how-rates-work/Residential-Rates-Plan-Pricing.pdf. [Accessed: 02-Jul-2021].

[48] Skyscraper Center, "Cities by Number of 150m+ Buildings - The Skyscraper

Center," 2021. [Online]. Available: https://www.skyscrapercenter.com/cities?list=buildings-150. [Accessed: 12-Jul-2021].

[49] G. W. Leeson, "The Growth, Ageing and Urbanisation of our World," *J. Popul. Ageing*, vol. 11, no. 2, pp. 107–115, 2018.

[50] R. Mahtta, A. Mahendra, and K. C. Seto, "Building up or spreading out? typologies of urban growth across 478 cities of 1 million+," *Environ. Res. Lett.*, vol. 14, no. 12, 2019.

[51] K. M. G. Wong, "Vertical cities as a solution for land scarcity: The tallest public housing development in Singapore," *Urban Des. Int.*, vol. 9, no. 1, pp. 17–30, 2004.

[52] V. A. Akristiniy and Y. I. Boriskina, "Vertical cities-the new form of high-rise construction evolution," *E3S Web Conf.*, vol. 33, pp. 1–11, 2018.

[53] M. Gormley, D. Kelly, D. Campbell, Y. Xue, and C. Stewart, "Building drainage system design for tall buildings: Current limitations and public health implications," *Buildings*, vol. 11, no. 2, pp. 1–17, 2021.

[54] C. Heinrich, C. Ziras, T. V. Jensen, H. W. Bindner, and J. Kazempour, "A local flexibility market mechanism with capacity limitation services," *Energy Policy*, vol. 156, p. 112335, Sep. 2021.

[55] C. Cid, Y. Qu, and M. R. Hoffmann, "Design and preliminary implementation of onsite electrochemical wastewater treatment and recycling toilets for the developing world," *Environ. Sci. Water Res. Technol.*, vol. 4, no. 10, pp. 1439–1450, 2018.

[56] Y. Zhang, S. Kusch-Brandt, S. Gu, and S. Heaven, “Particle size distribution in municipal solid waste pre-treated for bioprocessing,” *Resources*, vol. 8, no. 4, 2019.

[57] E. Parker, A. S. Germain, and E. S. Laurent, “A Study of Waste Water Energy Recovery and its Implementation in the Commonwealth of Massachusetts,” 2013.

[58] T. Lestina, “Heat Exchangers Fouling, Cleaning and Maintenance,” in *Handbook of Thermal Science and Engineering*, F. A. Kulacki, Ed. Cham: Springer International Publishing, 2017, pp. 1–33.

[59] A. Poullikkas, “A review of net metering mechanism for electricity renewable energy sources,” *Int. J. Energy Environ.*, vol. 4, no. 6, pp. 975–1002, 2013.

[60] “The Rooftop Pool: Is it Right for Your Hotel? - Base4.” [Online]. Available: https://www.base-4.com/rooftop-pool/. [Accessed: 03-May-2021].

[61] “Trucks Handbook.” [Online]. Available: http://www.mto.gov.on.ca/english/trucks/handbook/section1-3-7.shtml. [Accessed: 03-May-2021].

[62] P. Breeze, *Hydropower*. London: Academic Press, 2018.

[63] K. Yokoyama, M. Okazaki, and T. Komito, “Effect of contact pressure and thermal degradation on the sealability of O-ring,” *JSAE Rev.*, vol. 19, no. 2, pp. 123–128, 1998.

[64] Y. Demirel, “Energy Conservation,” in *Comprehensive Energy Systems*, vol. 5–5, Elsevier Inc., 2018, pp. 45–90.

[65] J. Duquette, “Thermofluids & Energy syst. design: Lecture 6 : Piping Systems,” Carleton University, Ottawa, 2020.

[66] A. McDonald and H. Magande, *Introduction to Thermo-Fluids Systems Design*, 1st ed. John Wiley & Sons, Ltd, 2012.

[67] J. Davis, Ed., *Metals Handbook*, 2nd ed. ASM International Handbook Committee, 1998.

[68] M. C. A. Schwedler, M. M. Hydeman, S. S. Hanson, S. V Skalko, R. V Heinisch, N. B. Heminger, J. F. Hogan, P. A. Baselici, J. Humble, H. M. Kaplan, J. G. Boldt, M. D. Lane, R. Lord, R. Burton, R. F. Mcgowan, and K. I. Emerson, *ASHRAE Standard: Energy Standard for Buildings Except Low-Rise Residential Buildings*. Atlanta, GA: American Society of Heating, Refrigerating and Air-Conditioning Engineers, Inc., 2010.

[69] S. Hagerman, "No Title," Carleton University, 2021.

[70] W. Shen, X. Chen, J. Qiu, J. A. Hayward, S. Sayeef, P. Osman, K. Meng, and Z. Y. Dong, "A comprehensive review of variable renewable energy levelized cost of electricity," *Renew. Sustain. Energy Rev.*, vol. 133, no. August, p. 110301, 2020.

[71] D. Danaci, P. A. Webley, and C. Petit, "Guidelines for Techno-Economic Analysis of Adsorption Processes," *Front. Chem. Eng.*, vol. 2, no. January, pp. 1–11, 2021.

[72] G. A. Aggidis, E. Luchinskaya, R. Rothschild, and D. C. Howard, "The costs of small-scale hydro power production: Impact on the development of existing potential," *Renew. Energy*, vol. 35, no. 12, pp. 2632–2638, Dec. 2010.

[73] K. C. Wilson, G. R. Addie, and R. Clift, "Slurry transport using centrifugal pumps," 3rd ed., Springer Science+Business Media, Inc, 1992, pp. 338–352.

[74] "Price History," 2021. [Online]. Available: http://steelbenchmarker.com/history.pdf.

[75] K. Mongird, V. Viswanathan, P. Balducci, J. Alam, V. Fotedar, V. Koritarov, and B. Hadjerioua, “Energy Storage Technology and Cost Characterization Report | Department of Energy,” no. July, 2019.

[76] Ontario Energy Board, “Historical electricity rates | Ontario Energy Board,” 2021. [Online]. Available: https://www.oeb.ca/rates-and-your-bill/electricity-rates/historical-electricity-rates. [Accessed: 01-Apr-2021].

[77] Hunter Water Corporation, “Operating and maintenance cost estimating guideline,” p. 5, 2013.

[78] “Utility-scale battery storage costs decreased nearly 70% between 2015 and 2018 - Today in Energy - U.S. Energy Information Administration (EIA).” [Online]. Available: https://www.eia.gov/todayinenergy/detail.php?id=45596. [Accessed: 17-May-2021].

[79] Canada Energy Regulator, “Canada Energy Future 2020,” 2020.

[80] P. J. Hibbard, A. M. Okie, and P. G. Darling, “Demand Response in Capacity Markets: Reliability, Dispatch and Emission Outcomes,” *Electr. J.*, vol. 25, no. 9, pp. 14–24, 2012.

[81] “Capacity Auction.” [Online]. Available: https://www.ieso.ca/en/Sector-Participants/Market-Operations/Markets-and-Related-Programs/Capacity-Auction. [Accessed: 30-Jun-2021].

[82] F. Baumgarte, G. Glenk, and A. Rieger, “Business Models and Profitability of Energy Storage,” *iScience*, vol. 23, no. 10, p. 101554, 2020.

[83] W. Cole and A. W. Frazier, “Cost Projections for Utility-Scale Battery Storage : 2020 Update Cost Projections for Utility-Scale Battery Storage : 2020 Update,”

Golden, 2020.